## General Disclaimer

## One or more of the Following Statements may affect this Document

- This document has been reproduced from the best copy furnished by the organizational source. It is being released in the interest of making available as much information as possible.

- This document may contain data, which exceeds the sheet parameters. It was furnished in this condition by the organizational source and is the best copy available.

- This document may contain tone-on-tone or color graphs, charts and/or pictures, which have been reproduced in black and white.

- This document is paginated as submitted by the original source.

- Portions of this document are not fully legible due to the historical nature of some of the material. However, it is the best reproduction available from the original submission.

# NASA Contractor Report 158958

(NASA-CR-158958) PRELIMINARY DESIGN CHARACTERISTICS OF A SUBSONIC BUSINESS JET CONCEPT EMPLOYING LAMINAR FLOW CONTROL (Vought Corp., Hampton, Va.) 48 p HC A03/MF A01 CSCL 01C G3/05

N78-33087

Unclas 33827

# PRELIMINARY DESIGN CHARACTERISTICS OF A SUBSONIC BUSINESS-JET CONCEPT EMPLOYING LAMINAR FLOW CONTROL

R. V. Turriziani, W. A. Lovell, J. E. Price,
C. B. Quartero, and G. F. Washburn

VOUGHT CORPORATION
HAMPTON TECHNICAL CENTER
Hampton, Virginia, 23666

CONTRACT NAS1-13500

September 1978


National Aeronautics and
Space Administration

**Langley Research Center**
Hampton, Virginia 23665

## SUMMARY

A study was conducted to determine the advantages of laminar flow control on an advanced subsonic business jet aircraft designed for transatlantic operation. The design mission was 5.93 Mm (3 200 n.mi.). Aircraft configurations were developed with laminar flow control (LFC) and without LFC. The LFC configuration had approximately eleven percent less parasite drag and a seven percent increase in the maximum lift-to-drag ratio. Although these aerodynamic advantages were partially offset by the additional weight of the LFC system, the LFC aircraft burned from six to eight percent less fuel for comparable missions. For the transatlantic design mission with the gross weight fixed, the LFC configuration would carry a greater payload for ten percent less fuel per passenger mile.

## INTRODUCTION

The objective of the study was to determine the effect of laminar flow control (LFC) on the design characteristics of a subsonic business jet sized for transatlantic range. The criteria and assumptions used in the study included a design range of 5.93 Mm (3 200 n.mi.) with reserves corresponding to the fuel required for a 45 minute flight extension. The maximum cruise Mach number was specified as 0.8. The aircraft is configured for a flight crew of 2 and accommodations for a maximum of 13 passengers.

Two aircraft configurations were developed; one with LFC and the other without for comparison purposes. The two aircraft were otherwise configured with the same engine, fuselage, and empennage sizes and for equal maximum gross weight. The wings represented the only geometry differences between the two configurations.

The LFC aircraft wing had a supercritical airfoil specifically designed for LFC application. Laminar flow control was assumed on both the upper and lower surfaces except for the areas of the ailerons and flaps. No LFC was used on other parts of the airplane.

Both study configurations have two main powerplants which are mounted on the side of the aft fuselage. The LFC model will require a power source for operation of the suction system. This can either be accomplished by means of power extraction from the main engines (bleed or gears) or with separate power units. No detailed analysis was made of the suction pump and drive system. However, estimated weight and drag penalties based on wing pod-mounted drive and pump units were included in the evaluations of the LFC airplane.

The study included configuration definition and layout, weight and drag estimations, development of an engine data deck for the mission analysis computer program, evaluation of the required suction power for wing laminarization, and mission performance analysis. Trade studies were conducted with payload (number of passengers), range, climb and cruise velocities, engine size, and passenger accommodations as variables. Additional studies were conducted to determine the effects on performance of engine size, aircraft size, and increased wing aspect ratio.

## SYMBOLS AND DEFINITIONS

Values are given in both the International System of Units (SI) and U.S. Customary Units. The calculations were made in U.S. Customary Units.

| | |
|---|---|
| AR | aspect ratio |
| c | chord length |
| $C_D$ | drag coefficient, Drag/qS |
| $C_{D_i}$ | induced drag coefficient |
| $C_{D_{P_{min}}}$ | minimum parasite drag coefficient |
| $C_f$ | average skin friction coefficient based on component wetted area |
| $C_L$ | lift coefficient, Lift/qS |

| | |
|---|---|
| $C_p$ | pressure coefficient |
| $C_{SP}$ | suction power coefficient based on reference wing area |
| $C_{SP_{airfoil}}$ | suction power coefficient based on chord length |
| $C_{SP_{local}}$ | suction power coefficient at a point on airfoil surface, based on unit area |
| LFC | laminar flow control |
| M | Mach number |
| MAC | mean aerodynamic chord |
| OWE | operating weight empty |
| p | pressure |
| q | dynamic pressure |
| $R_e$ | Reynolds number |
| s | distance along airfoil surface from stagnation point |
| S | reference wing area |
| T | thrust |
| V | true velocity |
| W | aircraft weight |
| $\Delta C_{D_M}$ | compressibility drag rise increment due to Mach number |
| $\Delta C_{D_p}$ | parasite drag increment as a function of lift |
| $\rho$ | air density |

Subscripts:

| | |
|---|---|
| w | at or into surface (wall) |
| $\infty$ | free stream |

## AIRCRAFT DEVELOPMENT

### Configuration Description

The two business jets configured for this study are assumed to incorporate the same size engine, fuselage, and empennage. One configuration includes an LFC system which resulted in differences in the wing geometry. Both airplanes are low-wing designs with two engines attached to the aft fuselage and with the horizontal stabilizer mounted on the vertical fin. A general arrangement of the aircraft without LFC is presented in figure 1 and a plan-view of the LFC version is shown in figure 2. Table I contains the geometric characteristics of the two configurations.

The identical fuselages for both aircraft accommodate a crew of 2 and a maximum of 13 passengers with a 86 cm (34 in.) seat pitch. The fuselage length is 16.46 m (54 ft) and the maximum diameter is 1.83 m (6 ft). The passenger cabin includes a toilet, a vanity cabinet, and a refreshment console. The center cabin aisle height is 152 cm (60 in.). A luggage compartment with a volume of 1.23 $m^3$ (43.5 $ft^3$) is located in the aft fuselage.

The landing gear of both airplanes has a single-wheel nose strut and two double-wheel main struts. The latter are mounted in the wing and retract into cavities below the cabin floor.

A supercritical airfoil with a thickness-chord ratio of 13 percent was selected for the configuration without LFC. This wing is swept 23° at the quarter chord, which results in a streamwise thickness ratio of 12 percent. The thickness ratio is constant over the wing span including those portions of the wing which have leading- and trailing-edge extensions. The wing has a reference area (trapezoidal) of 27.03 $m^2$ (291 $ft^2$) with a taper ratio of .388 and an aspect ratio of 9.77.

For the aircraft with laminar flow control, an airfoil section designated YNZE, developed by NASA for LFC applications, was selected with a

thickness-chord ratio of 14 percent. This slightly thicker wing has a quarter-chord sweep of 25° resulting in a streamwise thickness ratio of 12.7 percent. The LFC wing includes an inboard trailing-edge extension, but the desired laminarization precludes the addition of the leading-edge fairing used in the non-LFC configuration because of possible leading-edge boundary-layer instabilities. The thickness ratio is constant over the wing span. The reference wing area, taper ratio, and aspect ratio are the same as for the non-LFC wing design.

Pods to house units to provide the suction power for laminarization are mounted on the lower surface of each wing panel of the LFC configuration. The pods were scaled from pods used in a study conducted by a system contractor to the NASA Aircraft Energy Efficiency (ACEE) Program. The pods for the LFC configuration are 1.836 m (72.3 in.) long with a maximum diameter of .277 m (10.9 in.).

Both wings were assumed to have trailing-edge flaps and ailerons aft of approximately 75 percent of the wing chord but no leading-edge high-lift devices.

The empennage was sized based on tail volume coefficients of .72 for the horizontal tail and .06 for the vertical fin. These values approximate those of existing subsonic jets in the same gross weight class. These values resulted in a horizontal tail area of 4.83 $m^2$ (53 $ft^2$) and a vertical fin area of 3.90 $m^2$ (42 $ft^2$). No stability and control analyses were conducted to verify these results.

## Powerplant

The Garrett Airesearch TFE-731-2-2B turbofan engine, rated at 15.6 kN (3 500 lbf) thrust, was selected for both of the airplanes in this study. This rated thrust is the uninstalled take-off value of sea level static thrust for standard day conditions. Powerplant performance data for use in the aircraft mission analysis program, was generated from available performance

data for this engine.

The TFE-731-2-2B data (ref. 1) was corrected for the installation effects of inlet ram-pressure recovery and provided extraction of service airbleed by the methods provided in reference 2. This data was then scaled to the required thrust level 16.5 kN (3 700 lbf) within the mission analysis computer program.

## Fuel Capacities

The configuration without LFC incorporated a fuel tank in the wing box (including the carry through) with a capacity of 2.41 Mg (5 310 lbm). The leading-edge extension of this wing contained an additional tank with a capacity of 380 kg (830 lbm). The total wing fuel is thus 2.79 Mg (6 140 lbm). A fuselage tank with a capacity of 660 kg (1 460 lbm) is installed in the available space behind the passenger compartment. Therefore, a total of 3.45 Mg (7 600 lbm) of fuel can be carried by the airplane without LFC.

The configuration with LFC incorporated a wing box tank with 2.42 Mg (5 340 lbm) capacity plus the same size fuselage tank as on the aircraft without LFC. These tanks provided a total fuel capacity of 3.08 Mg (6 800 lbm). The reason for the lower fuel capacity is the absence of the leading-edge tank in the LFC wing.

As shown above, the wing-box capacities are nearly equal for both configurations. The maximum thickness-chord ratio of the LFC airfoil is somewhat larger than that of the airfoil selected for the configuration without LFC; however, the volumetric efficiency of the LFC airfoil is less because of the indented lower contour behind the leading edge and the volume required for the LFC skin structure, ducting, and other equipment.

As a result, the available tank space is 85 percent of the wing box volume for the LFC aircraft and 90 percent for the aircraft without LFC. Consequently, the rear spar was relocated from 65 percent to 70 percent on

the LFC version in order to achieve nearly equal wing-box fuel capacities for both of the aircraft.

## Weight and Balance

An aircraft performance analysis showed that the LFC airplane carrying 9 passengers would meet the desired 5.93 Mm (3 200 n.mi.) design range with maximum fuel of 3.08 Mg (6 800 lbm). The gross weight required to fly this mission was found to be 86.30 kN (19 400 lbf).

The operating weight empty of the LFC aircraft was estimated to be 49.82 kN (11 200 lbf) at a gross weight of 86.30 kN (19 400 lbf). These weights include accommodations for the maximum number of passengers (13), 2 crew members, and the extra weight of the LFC system. For the determination of the LFC system weight, a specific (or unit) weight of 93.83 $N/m^2$ (1.96 $lbf/ft^2$) of projected laminarized area was used. This value was obtained from studies conducted by system contractors to the NASA Aircraft Energy Efficiency Program. The laminarization on the wing extends on both upper and lower surfaces from the leading edge to approximately 75 percent of the chord, and spanwise from the sides of the fuselage to the wing tips. The projected area of this laminarized surface measures 17.09 $m^2$ (184 $ft^2$), resulting in a LFC weight penalty of approximately 1.60 kN (360 lbf). The weight of the passenger accommodations (seats, oxygen, etc.) was estimated to be 445 N (100 lbf) per passenger. The non-LFC configuration has larger wing tanks. Their weight is reflected in the propulsion system weight. For the LFC version the weight of the wing mounted pods is included in the LFC system specific weight value, therefore, it is accounted for in the structural wing weight.

The aircraft without LFC was assumed to have an equal maximum gross weight of 86.30 kN (19 400 lbf). The corresponding operating weight empty is 48.04 kN (10 800 lbf) including accommodations for 13 passengers and 2 crew members. Weight breakdowns for the two models are presented in tables II and III for varying numbers of passengers and the corresponding

passenger accommodations. Mission fuel is limited by the gross weight for the 9 and 13 passenger variations and by maximum fuel for the 5 passenger variations.

A cursory analysis indicated a center of gravity travel from approximately 16 percent to 31 percent of the MAC on both aircraft which is typical of this class of aircraft.

## AERODYNAMIC ANALYSIS

### LFC Suction Power

The theoretical suction power required for laminarization of the LFC wing upper and lower surfaces from the leading edge to the hinge lines of the flaps and ailerons (approximately 75 percent of wing chord) was computed. This suction power was determined, in coefficient form, for the average long-range cruise and average high-speed cruise conditions. The conditions for long-range cruise were an altitude of 14.6 km (48 000 ft), a lift coefficient of .62, and a unit Reynolds number of 3.041 x $10^6/m^2$ (.9276 x $10^6/ft^2$) at M = .71. For the high-speed cruise, the conditions were an altitude of 13.4 km (44 000 ft), a lift coefficient of .40, and a unit Reynolds number of 4.150 x $10^6/m^2$ (1.265 x $10^6/ft^2$) at M = .80.

The suction power coefficient at any point on the LFC surface (ref. 3) is defined as

$$C_{SP_{local}} = \left[ \frac{\rho_w V_w}{\rho_\infty V_\infty} - C_p \cdot \frac{V_w}{V_\infty} \right]$$

System losses such as those in pumps, ducts, and valves are not accounted for.

The pressure coefficient distribution along the airfoil surface was computed with a two-dimensional transonic analysis program (ref. 4 and 5). The surface density ($\rho_w$) and suction flow velocity ($V_w$) distribution

were computed with the STAYLAM boundary layer program (ref. 6). The chordwise pressure distributions for the two cruise conditions are presented in figures 3 and 4, the density ratio distribution in figures 5 and 6, and the velocity ratio distribution in figures 7 and 8.

The chordwise distribution of the suction power coefficient along the upper and lower airfoil contours is shown in figures 9 and 10 for the two average cruise Mach numbers. The power coefficient distribution curves were integrated to obtain a power coefficient ($C_{SP_{airfoil}}$) based on total chord per unit span, for each Mach number.

The power coefficient, $C_{SP}$, for the laminarized part of the wing (based on total reference wing area) was determined through spanwise integration of the product of local chord length and $C_{SP_{airfoil}}$ values. This spanwise integration extended from the sides of the fuselage to the wing tips. The effects of the finite wing planform on the spanwise lift coefficient distribution were ignored. The values of the power coefficient resulting from the above integration were .00154 for M = .71 and .00133 for M = .80.

The coefficient $C_{SP}$ can be considered to represent either power or equivalent drag, depending on whether it is dimensionalized using $1/2\rho_\infty V_\infty^3 S$ for power or $1/2\rho_\infty V_\infty^2 S$ for drag. In this study, the $C_{SP}$ values were added to the aerodynamic drag of the aircraft. The equivalent suction drag actually depends upon lift coefficient and Reynolds number. However, since its magnitude is not too large, only the values at average cruise conditions were calculated. These values were assumed to be constant throughout the analysis.

## Drag Polars

Drag polars were generated for both the long range and high speed conditions. The drag polar is defined by the following equation:

$$C_{D_{total}} = C_{D_{P_{min}}} + \Delta C_{D_P} + C_{D_i} + \Delta C_{D_M} + C_{SP}$$

The value of the minimum parasite drag ($C_{D_{P_{min}}}$) was determined using methods developed by the Vought Corporation, Hampton Technical Center. Since this method was developed for only turbulent flow, corrections were applied to the results to account for the laminar portions of the LFC aircraft wing. The values of $C_{D_{P_{min}}}$ were adjusted on both aircraft for the Reynolds numbers corresponding to the various speed and altitude combinations encountered during climb and cruise.

Tables IV and V show the various components of the minimum parasite drag ($C_{D_{P_{min}}}$) as computed for the two study configurations. Drag coefficients are obtained by dividing the equivalent flat plate area values presented in the tables by the reference wing area of 27.03 $m^2$ (291 $ft^2$). Tables IV and V correspond to the start of high-speed cruise (M = .80) with the aircraft without LFC at 13.1 km (43 000 ft ) and the LFC airplane at 13.7 km (45 000 ft) altitude. Table V incudes both the turbulent and laminarized parasite drag values for the LFC aircraft wing including wing pods. The slight disparity between tables IV and V in the turbulent drag values for the airplane parts other than the wing is due to the difference in Reynolds numbers at the slightly different cruise altitudes.

A comparison of the two tables reveals a 57.5 percent reduction in wing parasite-drag flat-plate area due to laminarization [from .208 $m^2$ (2.24 $ft^2$) to .089 $m^2$ (.95 $ft^2$)]. However, the wing contributes only 34.2 percent to the total drag of the aircraft without LFC. The wing wetted area amounts to approximately 33 percent of the total wetted area. This percentage is comparable to that of the larger commercial passenger airplanes. Only 63 percent of the wing wetted area is laminarized since the flaps and ailerons are excluded. Furthermore, the addition of LFC introduces two new drag items, the equivalent suction drag and the drag of the suction engine pods. The net result is a

minimum parasite drag reduction for the entire airplane of only 11.3 percent (from $C_{D_{P_{min}}}$ = .02267 on the airplane without LFC to .01922 on the aircraft with LFC).

The variation of parasite drag with lift $\Delta C_{D_P}$, which includes angle-of-attack dependent friction drag, pressure drag, and the effects of a non-elliptical load distribution on the wing, is determined from correlations with jet transport flight data.

The induced drag $C_{D_i}$ was assumed to be $\frac{C_L^2}{\pi AR}$, which is the induced drag coefficient of a wing assuming an elliptical loading. The effects of deviations from elliptical loading are included in the flight correlations from which $\Delta C_{D_P}$ was determined.

Available data on the two airfoils used in this study indicated that the compressibility drag component $\Delta C_{D_M}$ is zero for Mach numbers up to .80.

The equivalent drag corresponding to the theoretically required LFC suction power $C_{SP}$ has been discussed in the preceding section on LFC suction power.

Figure 11 presents the resulting lift-drag polars. For each of the two study airplanes, two polars are shown; one for high-speed cruise, and the other corresponding to long-range cruise. At high-speed cruise, M = .80, the maximum lift-to-drag ratio for the non-LFC configuration was determined to be 18.0 and for the LFC version 19.3. The drag difference between the two cruise modes is caused only by Reynolds number effects, since compressibility drag was assumed to be zero. Since $C_{D_{P_{min}}}$ is only part of the entire drag, the .00255 reduction obtained with LFC amounts to only 7 percent of the total drag experienced at long-range cruise.

Lift-drag ratios for the two configurations at long-range cruise speed and high-speed cruise were derived from the polars in figure 11 and are presented in figure 12. The values at which the aircraft operate are identified on both figures 11 and 12.

## PERFORMANCE ANALYSIS

### Take-Off and Landing Performance

Take-off and landing performance were not analyzed in this study since wing loading, thrust-to-weight ratio, and the high-lift system of the study configuration are similar to those of existing business jets all of which operate from relatively short field lengths.

### Payload-Range Performance

The payload-range performance of the study aircraft was evaluated for both long-range cruise and high-speed cruise conditions. Estimates were made of take-off and descent fuel and descent distance. For reserves, a fuel allowance sufficient for an additional 45 minute flight at the end of the planned range was included in the total fuel carried on the flight. This reserve fuel allowance is typical for aircraft in this class.

The climb to cruise altitude for both aircraft was conducted at a constant equivalent airspeed of 129 m/s (250 kts) until the desired cruise Mach number was reached. An investigation of variations in climb speed showed insignificant effects on range. The LFC aircraft was assumed to climb with turbulent flow over the wing to an altitude at which the unit Reynolds number has dropped below $6.56 \times 10^6$/m ($2 \times 10^6$/ft) where the laminarization is considered to have become fully effective.

Two methods of computing the payload (weight) were considered. In the first method it was assumed that the passenger accommodations would be adjusted for the number of passengers carried on the flight thus reducing

the empty weight 445 N (100 lbf) per uncarried passenger. In the other method, the accommodations were assumed constant and equal to that corresponding to the maximum seating capacity.

The lift-drag ratio plots in figure 12 show that both aircraft cruise at less than maximum values. This is caused by the low wing-loading of these airplanes which is necessary to achieve relatively short take-off and landing capability with a simple flap system. Figures 13 to 16 show the effect of cruise speed and payload on range. Maximum range occurs at long-range cruise speeds of M = .70 for the non-LFC aircraft and M = .72 for the LFC aircraft. A comparison of figures 13 and 14 for the configuration without LFC, and figures 15 and 16, for the LFC version, show that the range reduction due to an increase in cruise velocity is less on the LFC aircraft. One reason for this is that up to M = .8 no compressibility drag is experienced. Also, Reynolds number effects are less on a laminar surface than on a turbulent one. Another reason is that the LFC airplane, as a result of its lesser drag, achieves a higher cruise altitude and, therefore, flies at a larger $C_L$ (.463 at M = .80) than the configuration without LFC ($C_L$ = .406). This larger $C_L$ causes the LFC airplane to operate higher on the L/D curve (fig. 12) where the curve is less steep and where variations in $C_L$ have less effect. For example, figure 12 shows that for the aircraft without LFC the L/D reduction equals 12.6 percent from 16.7 at long-range cruise to 14.6 at M = .8. For the LFC airplane L/D decreases from 18.5 at long-range cruise condition (M = .72) to 17.1 at high-speed cruise (M = .80), a reduction of 7.6 percent.

The payload and range values from figures 13 through 16 corresponding to the maximum design speed (M = .80), and maximum range conditions (M = .70 to .72), were replotted on figures 17 and 18 as payload (passenger) range curves. Figure 17 applies to the case in which passenger accommodations were adjusted to fit the number of passengers, and figure 18 reflects accommodations for 13 passengers. With more passengers, and thus for shorter range values, the range difference between the two aircraft decreases. This decrease occurs because the drag reduction obtained with

laminar flow has less influence on the shorter range due to the lower ratio of cruise time, when the LFC system is effective, to total mission time. With the maximum number of passengers (13) the ranges of both airplanes are practically equal.

Figure 19 presents a comparison of the fuel burned, and the reserve fuel, as a function of the range for both airplanes. This figure corresponds to the long-range cruise passenger-range curve of figure 17. However, figure 19 shows that the LFC airplane still requires approximately 7 percent less fuel. With the same amount of fuel as on the non-LFC aircraft, the LFC airplane would have a longer range. However, for the LFC airplane, this would result in a heavier gross weight and a longer take-off field length. The payload-range plot in figure 17 and the fuel-range plot in figure 19 show that with 9 passengers and at long-range cruise speed that the LFC airplane has approximately two percent longer range and requires six percent less fuel than the non-LFC aircraft. The aircraft without LFC will not fly the full 5.93 Mm (3 200 n.mi.) design range with a 9 passenger plus baggage payload. The corresponding fuel per passenger mile is shown in figure 20. This shows that the LFC aircraft burns approximatley ten percent less fuel per passenger mile than the non-LFC aircraft. It should be noted that the number of passengers is decreasing as the range increases in figure 19 and 20 and that the number of passengers differs for the LFC and non-LFC curves for the same range. For the same payload and range, the LFC configuration burns six to eight percent less fuel than the configuration without LFC.

The net improvement in performance due to LFC on a business jet was restricted due to engine sizing requirements. To obtain relatively short take-off and landing distances with a simple flap system and to provide adequate wing fuel capacity, the business jets were designed with a low take-off wing-loading of 3.19 kPa (66.7 $lbf/ft^2$). This low value resulted in a high cruise altitude. To reach this altitude, and also to improve the take-off performance, an engine was selected that provided a take-off T/W of .38. The same fairly high thrust powerplant was used for the

non-LFC and laminar configurations since both versions operated with turbulent flow during take-off and climb to altitude. However, the LFC airplane required much less thrust during cruise due to the laminarization. This resulted in the operating point of the LFC aircraft, on the specific fuel consumption versus thrust plot, to move from the bucket to the backside of the curve where the specific fuel value increases with a reduction in thrust. The specific fuel consumption of the LFC configuration during cruise was, therefore, approximately one-half percent higher than that of the non-LFC airplane.

## SUPPLEMENTARY STUDIES

During the course of this study the effects of engine size, aircraft size, and aspect ratio on LFC aircraft performance were investigated.

### Engine Size Effects

A brief investigation was conducted to ascertain the effect of engine size on the range of the LFC airplane. Sea level thrusts of ±.89 kN (200 lbf), from the 16.5 kN (3 700 lbf) size powerplant, were considered. The effect of engine size on OWE and fuel quantity was accounted for. The offsetting effects of L/D and SFC, both of which increase with increasing engine size, resulted in an insigificant (less than one percent) variation in range with engine size. The 16.5 kN (3 700 lbf) engine size produced the longest range.

### Aircraft Size Effects

The effects of aircraft size on the benefits that could be obtained with LFC were assessed. A wide-bodied jet transport was used for this study. The larger dimensions and higher wing loading allows the wide-bodied jet to fly at lower altitudes and higher Reynolds number and, consequently, lower parasite drag coefficients than the business jet. Thus the parasite drag reduction of the entire airplane, obtained with LFC, was found to be fifteen

percent for the larger airplane compared with eleven percent for the business jet. An even larger improvement could be expected for a wide-bodied jet specifically configured for LFC.

For the wide-bodied jet, the empty weight penalty was found to be only two percent as compared to four percent for the business jet based on the same ratio of LFC weight to projected laminarized area. In general, the ratio of gross weight to empty weight increases with the size of the aircraft which would further reduce the effect of the LFC weight penalty with increase in airplane size.

The wide-bodied transports operate from longer runways, have more sophisticated high lift systems, and less fuel capacity limitations. Wing loading could be higher resulting in a lower cruise altitude and lower thrust-to-weight ratio. Therefore, the relatively smaller engines could operate closer to the optimum specific fuel consumption.

These factors indicate that an LFC system would have greater payoff on a wide bodied jet transport than on a business jet.

## Aspect Ratio Effects

The effects of an increase in aspect ratio from 9.77 to an arbitrary value of 12 was analyzed. The operating weight empty increases resulting from the higher aspect ratio were estimated to be 534 N (120 lbf) for the non-LFC configuration and 667 N (150 lbf) for the LFC version. The maximum lift-drag ratio improved by approximatley ten percent on both aircraft, but the optimum lift coefficients corresponding to the maximum lift-drag ratio also increased by the same percentage. This increase meant that the already high cruise altitudes would have to be even higher in order to fly at maximum L/D.

If adequate fuel capacity were available, the range values at long-range cruise speed and with 9 passengers as shown in figure 17 would increase

for both aircraft by approximately 5.5 percent due to the larger aspect ratio. Also the fuel burned would decrease by one-half percent. However, the larger aspect ratio would cause a fuel capacity reduction in the wing box of approximately 6.5 percent. As previously discussed, the LFC airplane with an aspect ratio of 9.77 has less total fuel capacity than the non-LFC version. For the long-range cruise range values with 9 passengers shown in figure 17 the LFC airplane required its maximum fuel capacity while the non-LFC configurations required approximately 95 percent of its available fuel volume. With an aspect ratio of 12, the non-LFC aircraft still experienced no fuel capacity limitations on a 9 passenger mission. However, the LFC configuration would not have enough fuel to benefit fully from the drag reduction with an aspect ratio increase. The range gain would, therefore, only be 2.3 percent instead of the 5.5 percent previously mentioned.

## CONCLUSIONS

A study was conducted to determine the effects of laminar flow control (LFC) on the characteristics of a subsonic business jet designed for transatlantic operation. In order to evaluate these LFC effects a comparison was made between an LFC aircraft and an advanced turbulent flow wing airplane of nearly identical size and geometry. The results show that:

1. The transatlantic design range objective of 5.93 Mm (3 200 n.mi.) can be met by the LFC airplane with 9 passengers if the trip is flown at long-range cruise speed (M = .72) and the passenger accommodations do not exceed that necessary for the 9 passengers carried. Under the same conditions, the non-LFC version is capable of flying this distance but with only 8 passengers. With accommodations installed for the maximum 13 passengers, the number of passengers drops to 7 for the LFC and 6 for the non-LFC configuration.

2. The LFC configuration requires approximately 10 percent less fuel per passenger mile than the aircraft without LFC for the design mission.

3. Approximately 11 percent reduction in parasite drag and 7 percent increase in maximum lift-drag ratio is achieved with laminarization. This aerodynamic advantage is partially offset due to the additional weight of the LFC system.

4. The LFC configuration provides less fuel storage capacity than the non-LFC version and requires all this fuel for the transatlantic mission. The aircraft without LFC needs more fuel for this range but the required fuel is still below its fuel maximum capacity.

5. The payload-range performance at long-range cruise speed and equal take-off gross weight indicates that the range advantage of the LFC aircraft over the non-LFC aircraft decreases with increasing payload (passenger) from approximately two percent with a payload of 9 passengers to essentially zero percent with 13 passengers.

6. Due to engine sizing requirements for relatively short airfields, the LFC aircraft cannot operate at the optimum SFC for cruise, thus limiting the performance payoff.

7. Increases in wing aspect ratio have a beneficial effect on range, however, the full benefits cannot be realized for the LFC aircraft primarily due to reduced fuel volume when compared to the non-LFC aircraft.

## REFERENCES


1. Brandys, E. L. and Viquesney, J. L.: 731 Turbofan Engine, Preliminary Installation Manual. IM-8001, 4 October 1971.

2. Clarke, P. J.: Performance Correction Procedure for Airesearch Model TFE-731-2-2B Turbofan Engine (Gates Learjet Corporation). PE-8119-R, 30 June 1970.

3. Lovell, W. A.; Price, J. E.; Quartero, C. B.; Turriziani, R. V.; and Washburn, G. F.: Design of a Large Span-Distributed Load Flying-Wing Cargo Airplane with Laminar Flow Control. NASA CR-145376, May 1978.

4. Bauer, Frances; Garabedian, Paul; Korn, David; and Jameson, Antony: Supercritical Wing Sections II. Volume 108 of Lecture Notes in Economics and Mathematical Systems, Springer-Verlag, 1975.

5. Bauer, Frances; Garabedian, Paul; and Korn, David: Supercritical Wing Sections III. Volume 150 of Lecture Notes in Economics and Mathematical Systems, Springer-Verlag, 1977.

6. Carter, James E.: STAYLAM: A FORTRAN Program for the Suction Transition Analysis of a Yawed Wing Laminar Boundary Layer. NASA TM X-74013, March 1977.

TABLE I. - SUBSONIC BUSINESS JET - PHYSICAL CHARACTERISTICS

| | Wing | Horizontal Tail | Vertical Tail |
|---|---|---|---|
| area (reference) - $m^2$ ($ft^2$) | 27.03 (291) | 4.83 (52) | 3.90 (42) |
| aspect ratio | 9.77 | 5.36 | 1.54 |
| taper ratio | .388 | .499 | .423 |
| sweep @ 1/4 chord - deg., LFC | 25 | 25 | 35 |
| non-LFC | 23 | | |
| thickness to chord ratio, LFC | .127 | .09 | .09 |
| non-LFC | .120 | | |
| span - m (ft) | 16.25 (53.33) | 5.09 (16.7) | 2.44 (8.0) |
| volume coefficient | - | .72 | .06 |

fuselage length - m (ft): 16.46 (54.0)
dia. - m (ft): 1.83 (6.0)
max. number of passengers: 13
powerplant - type: Garrett/Airesearch TFE-731-3
- thrust: 16.5 kN (3700 lbf) (max. un-installed take-off thrust @ sea level/standard day)
max. take-off gross weight = 86.30 kN (19 400 lbf)
take-off wing loading = 3.19 kPa (66.7 $lbf/ft^2$)

| | FUEL CAPACITIES | | | | | | | |
|---|---|---|---|---|---|---|---|---|
| | Wing box | | Wing L.E. Extension | | Fuselage | | Total | |
| | Mg | lbm | Mg | lbm | Mg | lbm | Mg | lbm |
| turbulent A/C | 2.41 | 5310 | .38 | 830 | .66 | 1460 | 3.45 | 7600 |
| LFC aircraft | 2.42 | 5340 | - | - | .66 | 1460 | 3.08 | 6800 |

NOTE: Unless indicated otherwise, values apply to both LFC and non-LFC aircraft.

TABLE II. - WEIGHT SUMMARY OF SUBSONIC BUSINESS JET WITHOUT LFC

| Number of passengers | 13 | | 9 | | 5 | |
|---|---|---|---|---|---|---|
| | kN | lbf | kN | lbf | kN | lbf |
| Structure | | | | | | |
| - excluding wing | 12.59 | 2830 | 12.59 | 2830 | 12.59 | 2830 |
| - wing | 7.34 | 1650 | 7.34 | 1650 | 7.34 | 1650 |
| Propulsion | 8.05 | 1810 | 8.05 | 1810 | 8.05 | 1810 |
| Systems | 17.26 | 3880 | 15.48 | 3480 | 1370 | 3080 |
| Weight empty | 45.24 | 10170 | 43.46 | 9770 | 41.68 | 9370 |
| Operating items | 2.80 | 630 | 2.80 | 630 | 2.80 | 630 |
| Operating weight empty | 48.04 | 10800 | 46.26 | 10400 | 44.48 | 10000 |
| Payload | 11.57 | 2600 | 8.01 | 1800 | 4.45 | 10000 |
| Zero fuel weight | 59.61 | 13400 | 54.27 | 12200 | 48.93 | 11000 |
| Mission fuel | 26.69 | 6000 | 32.03 | 7200 | 33.81 | 7600(max) |
| Take-off gross weight | 86.30 | 19400 | 86.30 | 19400 | 82.74 | 18600 |

NOTE: The passenger accommodations (seats, oxygen) are assumed to be adjusted for the number of passengers carried. This is reflected in the system weight values shown above.

TABLE III. - WEIGHT SUMMARY OF SUBSONIC BUSINESS JET WITH LFC.

| Number of passengers | 13 | | 9 | | 5 | |
|---|---|---|---|---|---|---|
| | kN | lbf | kN | lbf | kN | lbf |
| Structure | | | | | | |
| - excluding wing | 12.86 | 2890 | 12.86 | 2890 | 12.86 | 2890 |
| - wing | 8.36 | 1880 | 8.36 | 1880 | 8.36 | 1880 |
| Propulsion | 7.96 | 1790 | 7.96 | 1790 | 7.96 | 1790 |
| Systems | 17.84 | 4010 | 16.06 | 3610 | 14.28 | 3210 |
| Weight empty | 47.02 | 10570 | 45.24 | 10170 | 43.46 | 9770 |
| Operating items | 2.80 | 630 | 2.80 | 630 | 2.80 | 630 |
| Operating weight empty | 49.82 | 11200 | 48.04 | 10800 | 46.26 | 10400 |
| Payload | 11.57 | 2600 | 8.01 | 1800 | 4.45 | 1000 |
| Zero fuel weight | 61.39 | 13800 | 56.05 | 12600 | 50.71 | 11400 |
| Mission fuel | 24.91 | 5600 | 30.25 (max) | 6800 (max) | 30.25 (max) | 6800 (max) |
| Take-off gross weight | 86.30 | 19400 | 86.30 | 19400 | 80.96 | 18200 |

NOTE: The passenger accommodations (seats, oxygen) are assumed to be adjusted for the number of passengers carried. This is reflected in the system weight values shown above.

TABLE IV. - MINIMUM PARASITE DRAG - BUSINESS JET WITHOUT LFC

| Airplane Part | Wetted Area | Reynolds Number | Drag Item | Coeff. $C_f$ | Equivalent Flat Plate Area $m^2$ | Equivalent Flat Plate Area $ft^2$ |
|---|---|---|---|---|---|---|
| Wing | 52.76 $m^2$ (568 $ft^2$) | $7.55 \times 10^6$ | Uncorr. flat plate | .00289 | .152 | 1.64 |
| | | | Supervelocity | | .031 | .34 |
| | | | Pressure drag | | .002 | .02 |
| | | | Wing/Body interf. | | .006 | .07 |
| | | | Excrescences | | .012 | .13 |
| | | | Surface roughness | | .005 | .05 |
| | | | | | .208 | 2.24 |
| Horizontal Tail | 9.75 $m^2$ (105 $ft^2$) | $4.13 \times 10^6$ | Uncorr. flat plate | .00320 | .031 | .34 |
| | | | Supervelocity | | .005 | .05 |
| | | | Pressure drag | | .000 | .00 |
| | | | Interference | | .002 | .02 |
| | | | Excrescences | | .003 | .03 |
| | | | Surface roughness | | .001 | .01 |
| | | | | | .042 | .45 |
| Vertical Tail | 9.10 $m^2$ (98 $ft^2$) | $6.94 \times 10^6$ | Uncorr. flat plate | .00293 | .027 | .29 |
| | | | Supervelocity | | .004 | .04 |
| | | | Pressure drag | | .000 | .00 |
| | | | Interference | | .002 | .02 |
| | | | Excrescences | | .002 | .02 |
| | | | Surface roughness | | .001 | .01 |
| | | | | | .036 | .38 |
| Fuselage | 68.75 $m^2$ (740 $ft^2$) | $7.17 \times 10^7$ | Uncorr. flat plate | .00205 | .141 | 1.52 |
| | | | 3-dim. effect | | .001 | .01 |
| | | | Supervelocity | | .007 | .08 |
| | | | Pressure drag | | .001 | .01 |
| | | | Non-optimum shape | | .003 | .03 |
| | | | Cockpit drag | | .023 | .25 |
| | | | Pressurization | | .007 | .08 |
| | | | Excrescences | | .008 | .09 |
| | | | Surface roughness | | .005 | .05 |
| | | | | | .196 | 2.12 |

Table IV. - Concluded.

| Airplane Part | Wetted Area | Reynolds Number | Drag Item | Coeff. $C_f$ | Equivalent Flat Plate Area $m^2$ | Equivalent Flat Plate Area $ft^2$ |
|---|---|---|---|---|---|---|
| Engine Struts | 2.78 $m^2$ (30 $ft^2$) | $8.89 \times 10^6$ | Uncorr. flat plate | .00281 | .007 | .08 |
| | | | Supervelocity | | .001 | .01 |
| | | | Pressure drag | | .000 | .00 |
| | | | Excrescences | | .001 | .01 |
| | | | Surface roughness | | .001 | .01 |
| | | | | | .010 | .11 |
| Nacelles | 15.79 $m^2$ (170 $ft^2$) | $1.19 \times 10^7$ | Uncorr. flat plate | .00269 | .043 | .46 |
| | | | 3-Dim. effect | | .000 | .00 |
| | | | Supervelocity | | .013 | .14 |
| | | | Excrescences | | .009 | .09 |
| | | | Surface roughness | | .001 | .01 |
| | | | Loss of lip suct. | | .007 | .08 |
| | | | Boattail drag | | .007 | .08 |
| | | | Interference | | .028 | .30 |
| | | | | | .108 | 1.16 |
| Trim | | | | | .003 | .03 |
| Air conditioning, etc. | | | | | .005 | .05 |
| | | | | | .608 | 6.54 |

Based on projected wing area of 27.03 $m^2$ (291 $ft^2$):

$$C_{D_{p_{min}}} = \frac{.608}{27.03} = \frac{(6.54)}{(291)} = .02247$$

TABLE V. - MINIMUM PARASITE DRAG - BUSINESS JET WITH LFC

| Airplane Part | Wetted Area | Reynolds Number | Drag Item | Coeff. $C_f$ | Equivalent Flat Plate Area 100% turb. wing $m^2$ | 100% turb. wing $ft^2$ | 75% lam. wing $m^2$ | 75% lam. wing $ft^2$ |
|---|---|---|---|---|---|---|---|---|
| Wing | 51.93 $m^2$ (559 $ft^2$) | 6.74 x $10^6$ | Uncorr. flat plate | .00295 | .153 | 1.65 | .064 | .69 |
| | | | Supervelocity | | .028 | .31 | .012 | .13 |
| | | | Pressure drag | | .003 | .03 | .001 | .01 |
| | | | Wing/Body interf. | | .007 | .07 | .007 | .07 |
| | | | Excrescences | | .006 | .06 | .003 | .03 |
| | | | Surface roughness | | .005 | .05 | .002 | .02 |
| | | | | | .202 | 2.17 | .089 | .95 |
| Horizontal Tail | 9.75 $m^2$ (105 $ft^2$) | 3.75 x $10^6$ | Uncorr. flat plate | .00326 | .031 | .34 | | |
| | | | Supervelocity | | .005 | .05 | | |
| | | | Pressure drag | | .000 | .00 | | |
| | | | Interference | | .002 | .02 | | |
| | | | Excrescences | | .003 | .03 | | |
| | | | Surface roughness | | .001 | .01 | | |
| | | | | | .042 | .45 | .042 | .45 |
| Vertical Tail | 9.10 $m^2$ (98 $ft^2$) | 6.31 x $10^6$ | Uncorr. flat plate | .00298 | .027 | .29 | | |
| | | | Supervelocity | | .004 | .04 | | |
| | | | Pressure drag | | .000 | .00 | | |
| | | | Interference | | .002 | .02 | | |
| | | | Excrescences | | .003 | .03 | | |
| | | | Surface roughness | | .001 | .01 | | |
| | | | | | .037 | .39 | .037 | .39 |
| Fuselage | 68.75 $m^2$ (740 $ft^2$) | 6.51 x $10^7$ | Uncorr. flat plate | .00208 | .143 | 1.54 | | |
| | | | 3-dim. effect | | .001 | .01 | | |
| | | | Supervelocity | | .008 | .09 | | |
| | | | Pressure drag | | .001 | .01 | | |
| | | | Non-optimum shape | | .003 | .03 | | |
| | | | Cockpit drag | | .023 | .25 | | |
| | | | Pressurization | | .007 | .08 | | |
| | | | Escrescences | | .008 | .09 | | |
| | | | Surface roughness | | .005 | .05 | | |
| | | | | | .199 | 2.15 | .199 | 2.15 |

Table V. - Concluded.

| Airplane Part | Wetted Area | Reynolds Number | Drag Item | Coeff. $C_f$ | Equivalent Flat Plate Area 100% turb. wing $m^2$ | 100% turb. wing $ft^2$ | 75% lam. wing $m^2$ | 75% lam. wing $ft^2$ |
|---|---|---|---|---|---|---|---|---|
| Engine Struts | 2.79 $m^2$ (30 $ft^2$) | $8.08 \times 10^6$ | Uncorr. flat plate | .00286 | .008 | .09 | | |
| | | | Supervelocity | | .001 | .01 | | |
| | | | Pressure drag | | .000 | .00 | | |
| | | | Excrescences | | .001 | .01 | | |
| | | | Surface roughness | | .000 | .00 | | |
| | | | | | .010 | .11 | .010 | .11 |
| Nacelles | 15.79 $m^2$ (170 $ft^2$) | $1.09 \times 10^7$ | Uncorr. flat plate | .00273 | .044 | .48 | | |
| | | | 3-dim. effect | | .000 | .00 | | |
| | | | Supervelocity | | .013 | .14 | | |
| | | | Excrescences | | .008 | .09 | | |
| | | | Surface roughness | | .001 | .01 | | |
| | | | Loss of lip suct. | | .007 | .08 | | |
| | | | Boattail drag | | .007 | .08 | | |
| | | | Interference | | .028 | .30 | | |
| | | | | | .108 | 1.17 | .108 | 1.17 |
| Trim | | | | | .003 | .03 | .003 | .03 |
| Air conditioning, etc. | | | | | .005 | .05 | .005 | .05 |
| Suction engine pods | | | | | - | - | .010 | .11 |
| Equivalent suction drag | | | | | - | - | .036 | .39 |
| | | | | | .606 | 6.52 | .538 | 5.80 |

Based on projected wing area of 27.03 $m^2$ (291 $ft^2$):

Total airplane $C_{D_{P_{min}}}$ = .02241 with 100% turbulent wing

= .01992 with 75% laminar wing

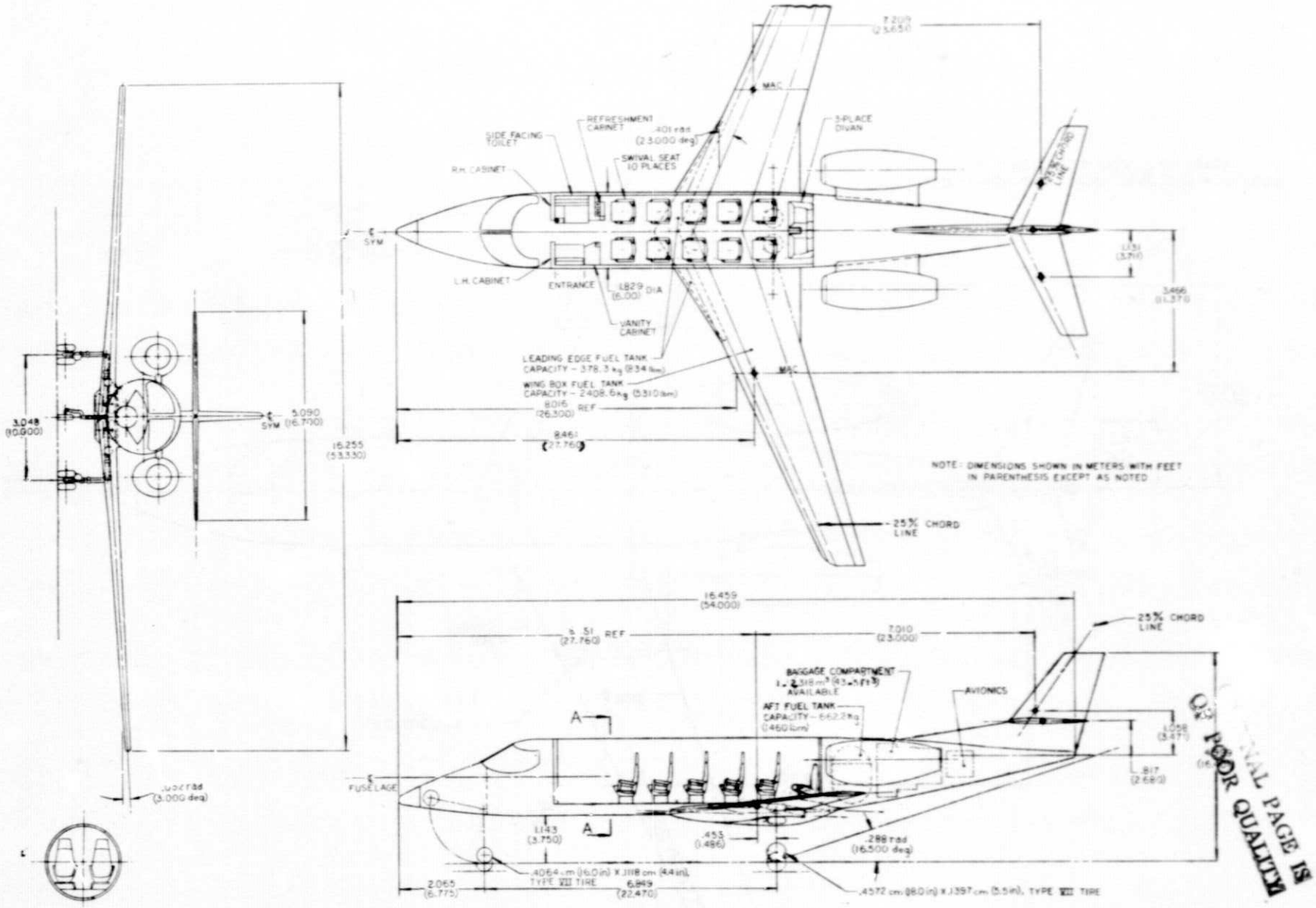


Figure 1. - General arrangement of business jet without LFC.

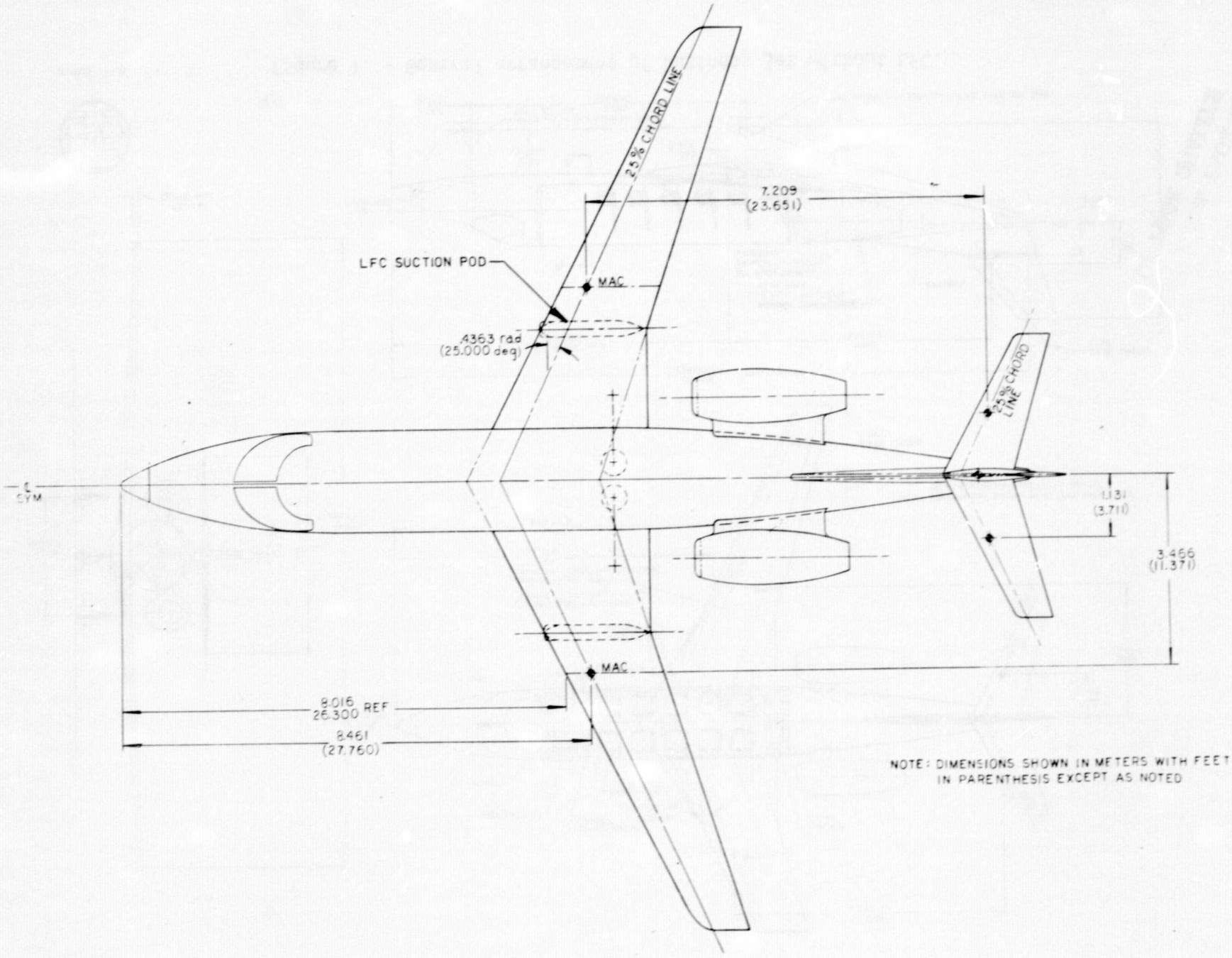


Figure 2. - Planform of business jet with LFC.

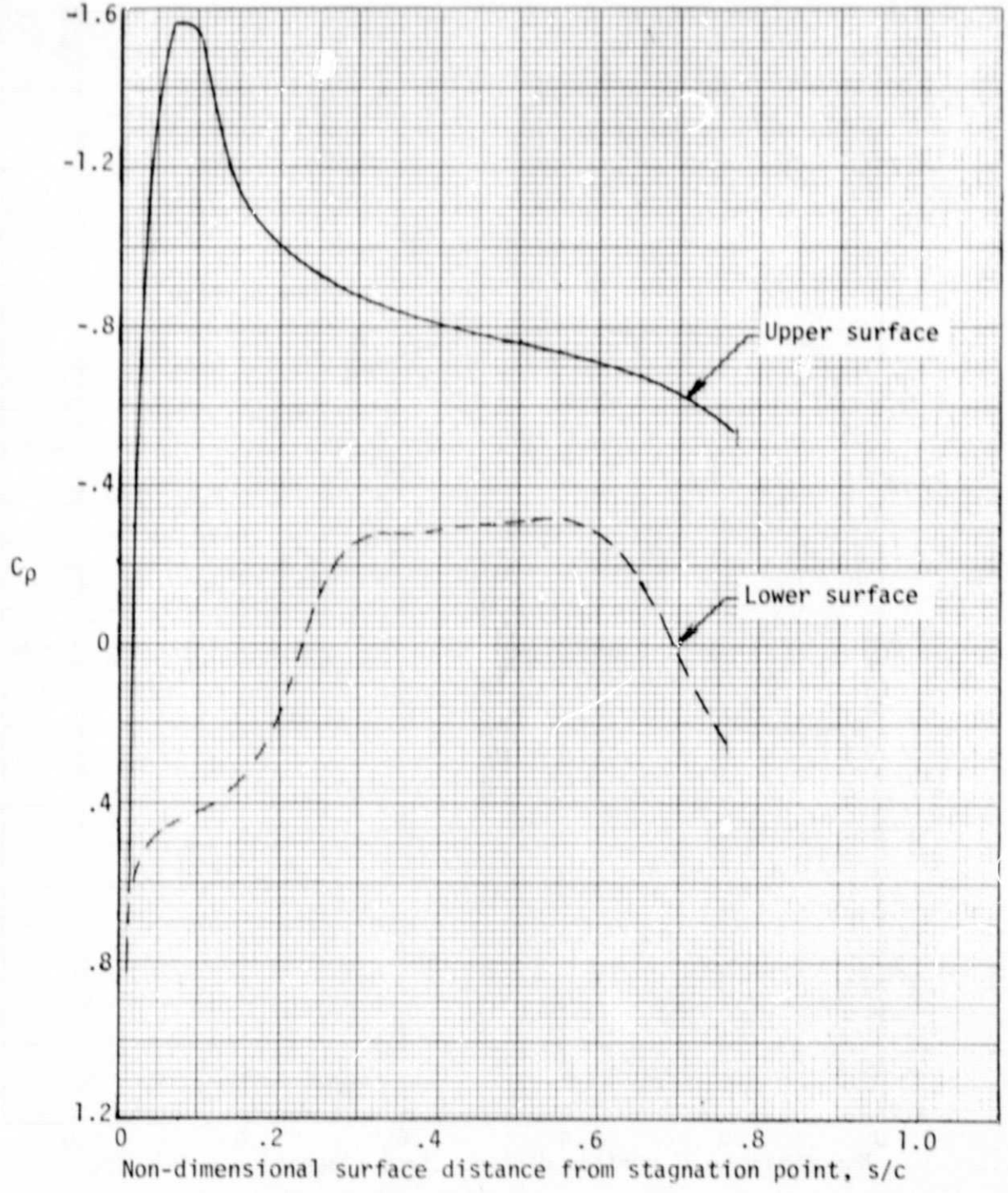


Figure 3. - Pressure distribution on YNZE airfoil with t/c = 12.7%, laminarized over 75% of the chord for M = .71 and $C_L$ = .62.

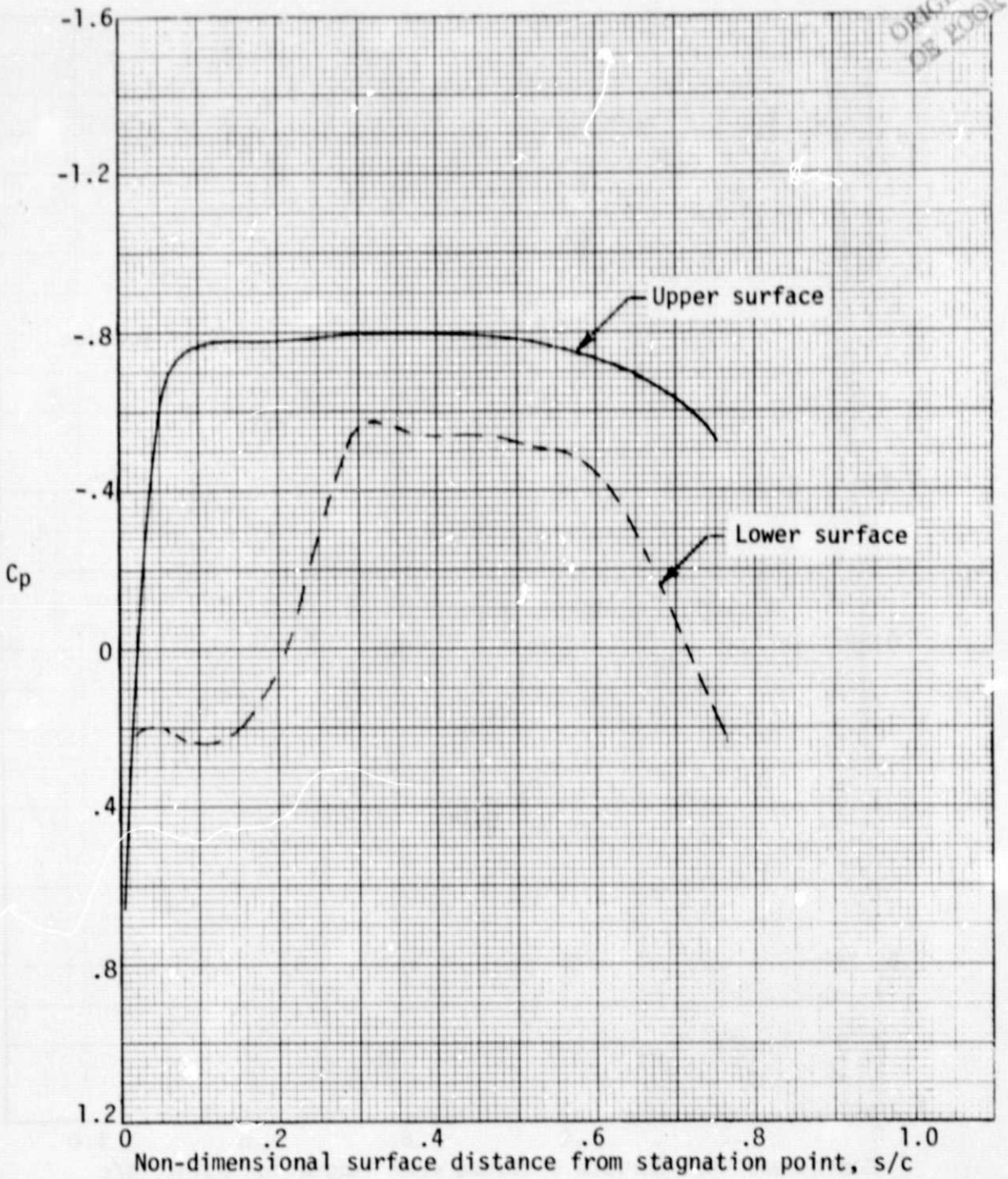


Figure 4. - Pressure distribution on YNZE airfoil with t/c = 12.7%, laminarized over 75% of the chord for M = .80 and $C_L$ = .40.

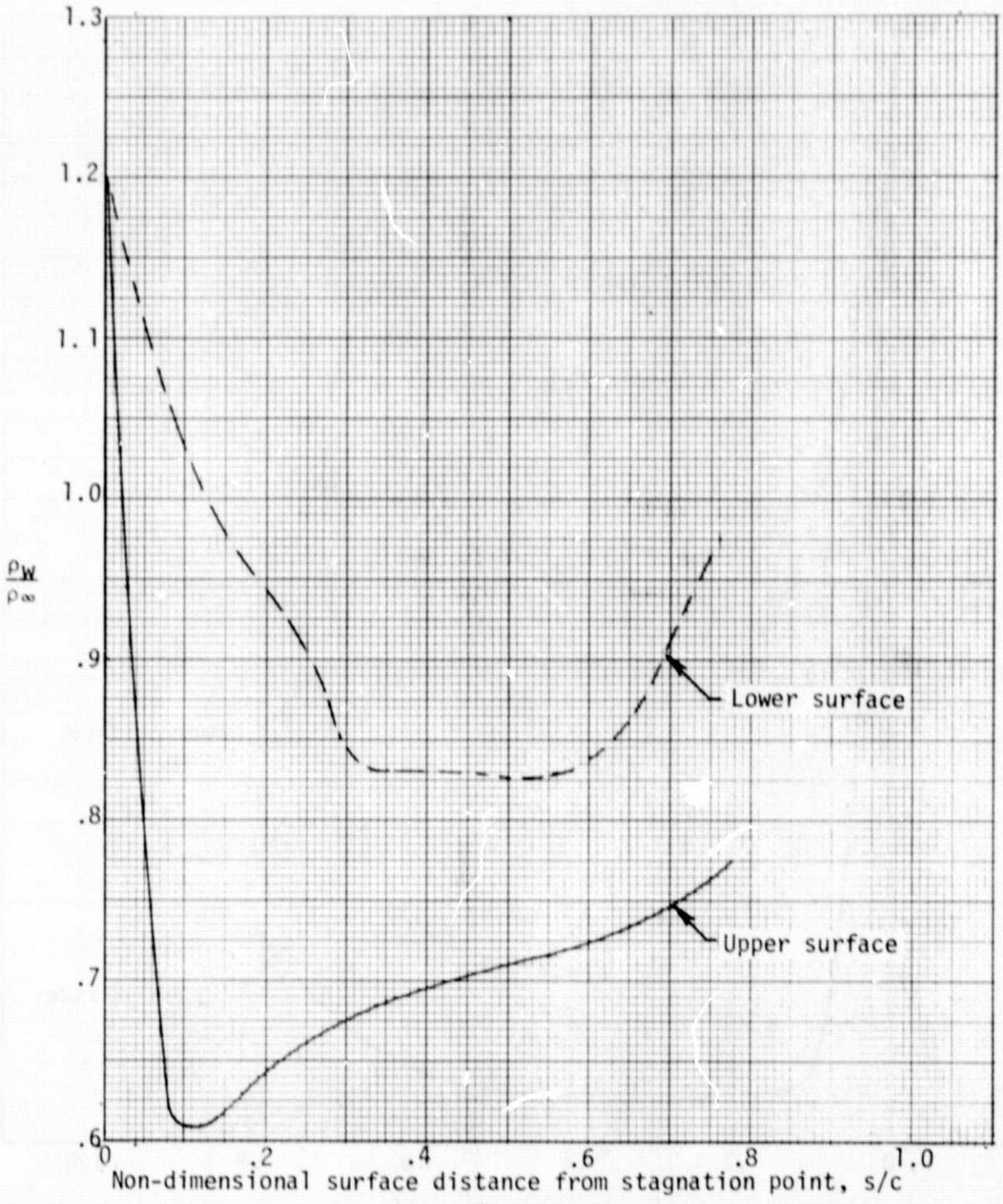


Figure 5. - Air density distribution along surface of YNZE airfoil with t/c = 12.7%, laminarized over 75% of the chord for M = .71 and $C_L$ = .62.

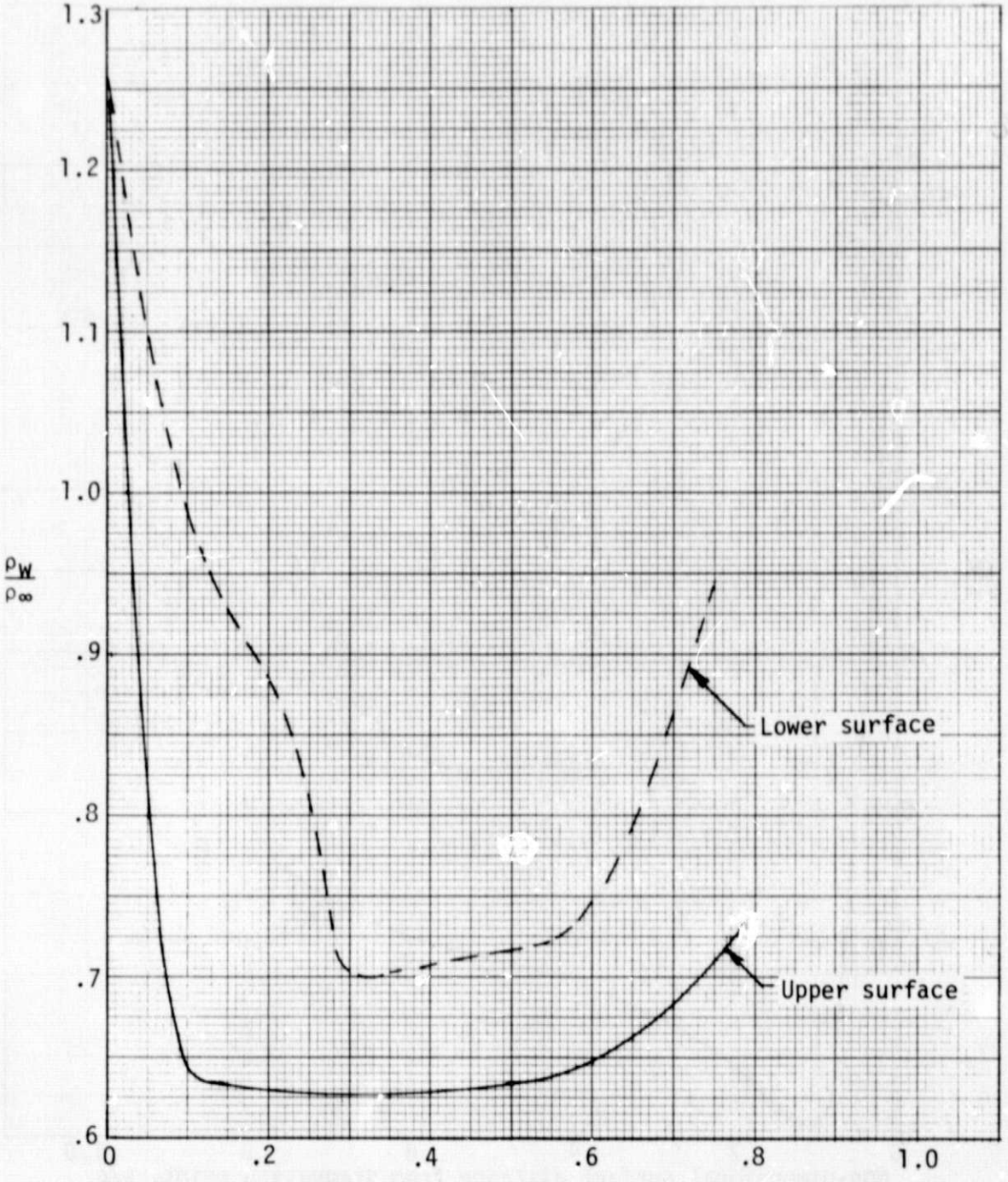


Figure 6. - Air density distribution along surface of YNZE airfoil with t/c = 12.7%, laminarized over 75% of the chord for M = .80 and $C_L$ = .40.

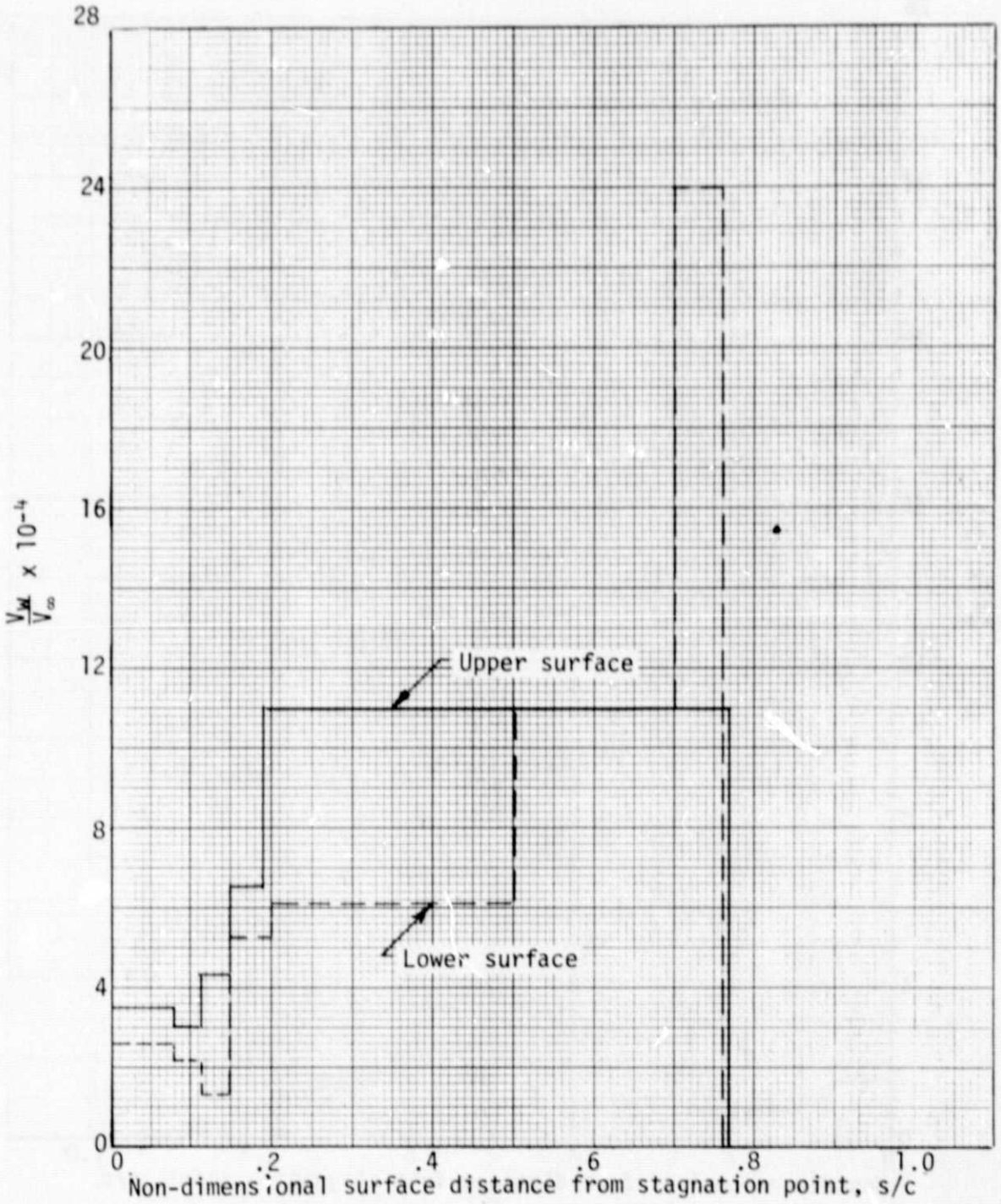


Figure 7. - Suction velocity distribution along surface of YNZE airfoil with t/c = 12.7%, laminarized over 75% of the chord for M = .71, $C_L$ = .62, and $R_e$ = 3.04 x $10^6$/m (.927 x $10^6$/ft).

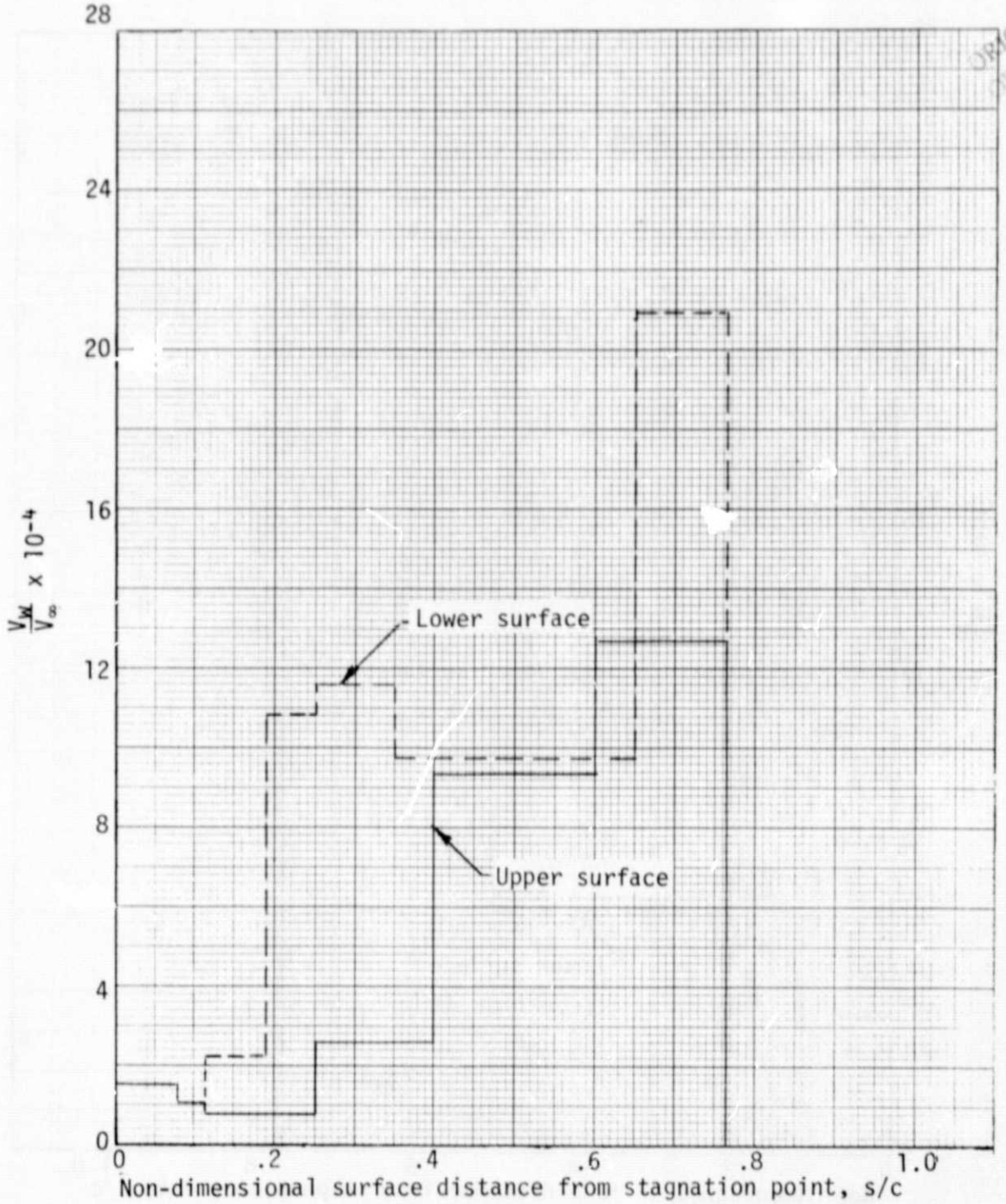


Figure 8. - Suction velocity distribution along surface of YNZE airfoil with t/c = 12.7%, laminarized over 75% of the chord for M = .80, $C_L$ = .40, and $R_e$ = 4.15 x $10^6$/m (1.265 x $10^6$/ft).

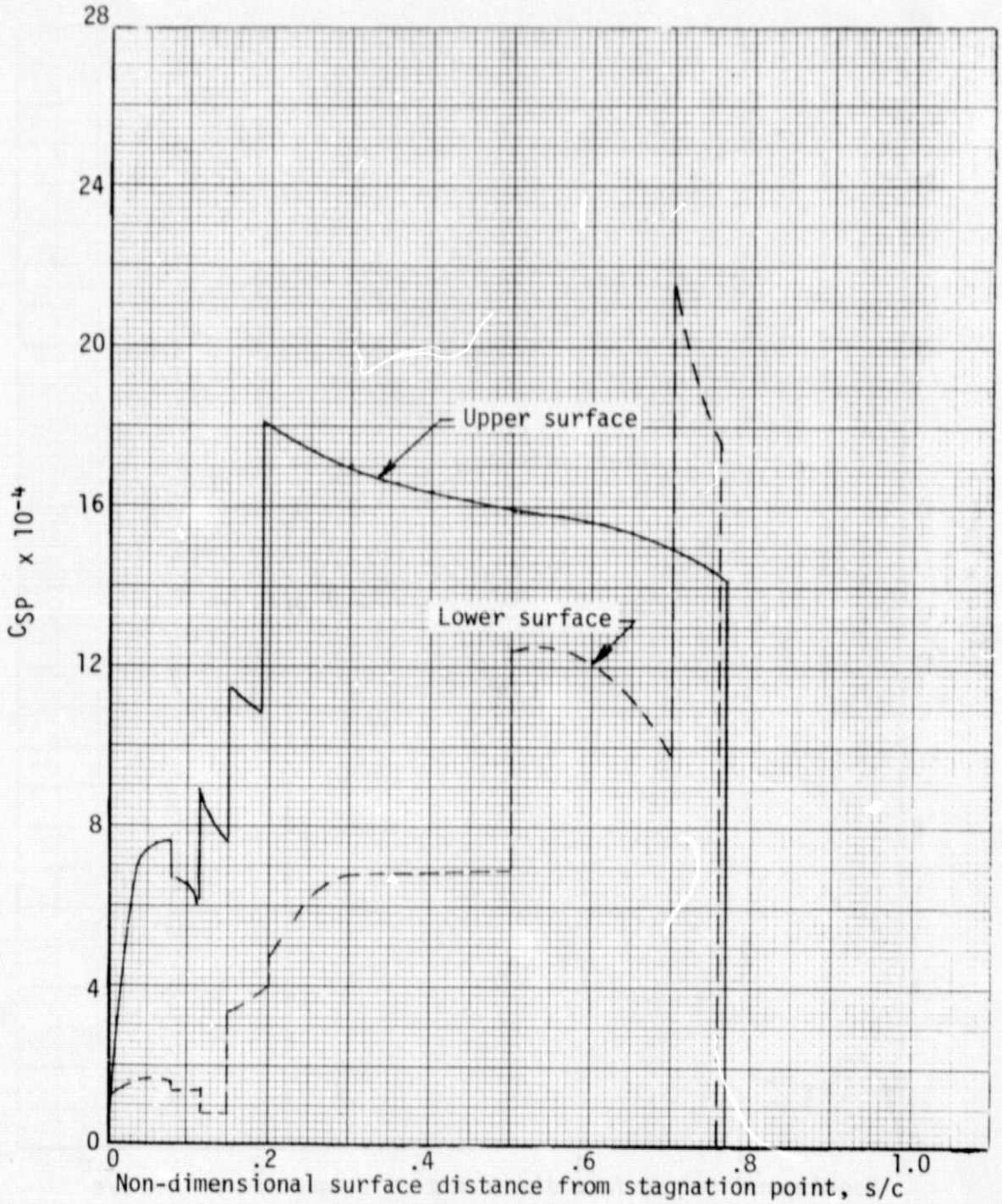


Figure 9. - Suction power coefficient distribution along surface of YNZE airfoil with t/c = 12.7%, laminarized over 75% of the chord for M = .71, $C_L$ = .62, and $R_e$ = 3.04 x $10^6$/m (.927 x $10^6$/ft).

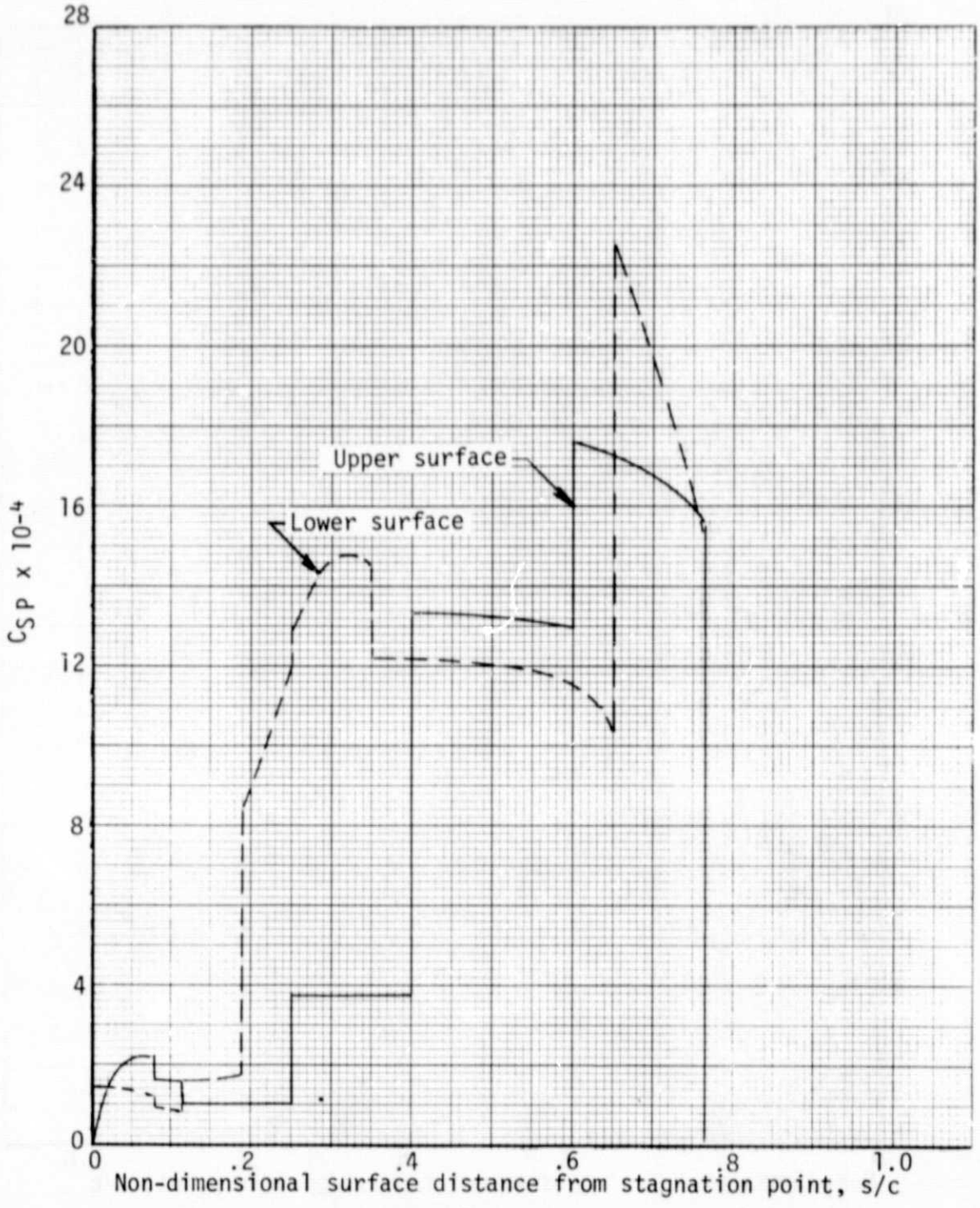


Figure 10. - Suction power coefficient distribution along surface of YNZE airfoil with t/c - 12.7%, laminarized over 75% of the chord for M = .80, $C_L$ = .40, and $R_e$ = 4.15 x $10^6$/m (1.265 x $10^6$/ft).

Figure 11. - Cruise drag polars

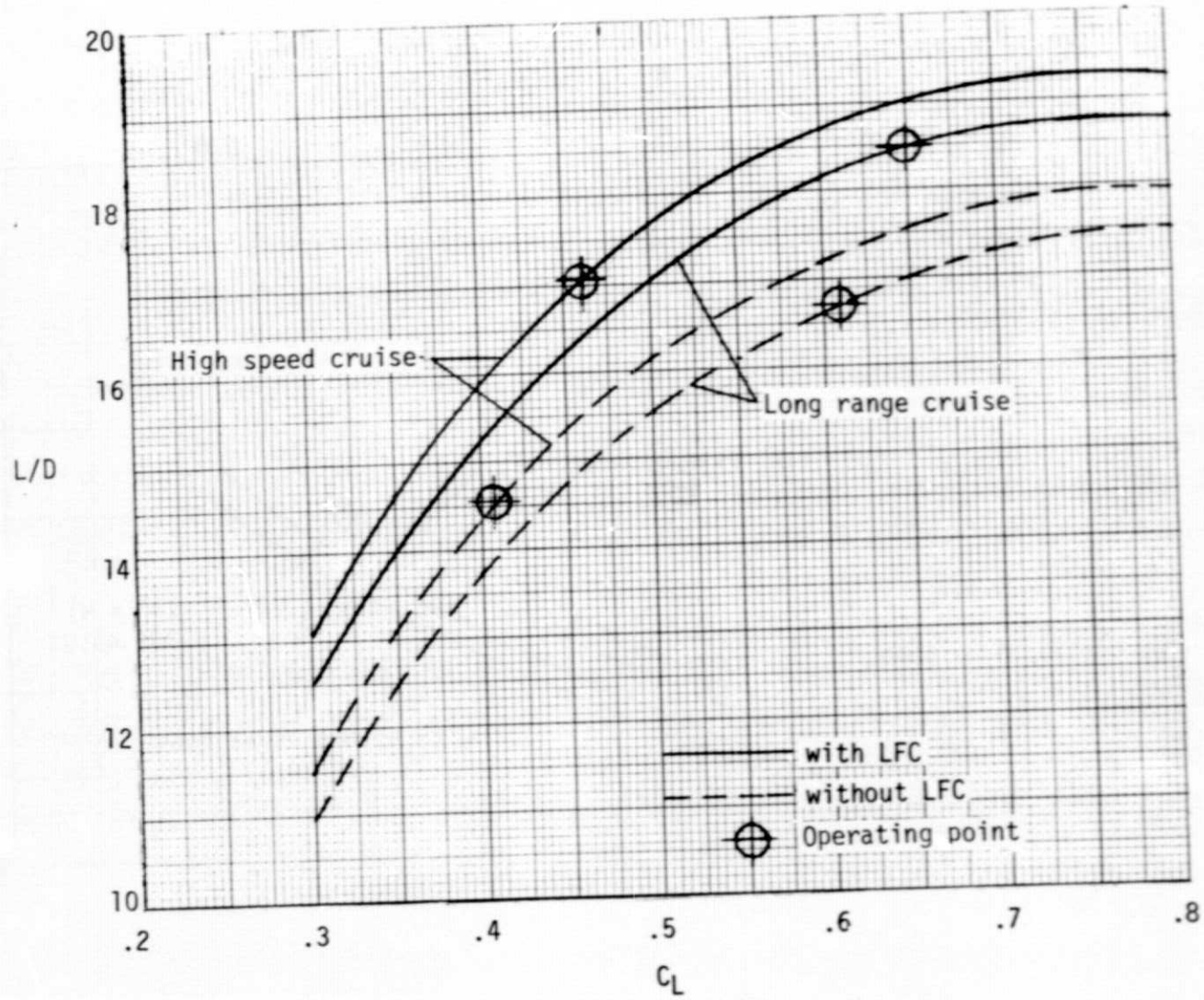


Figure 12. - Lift to drag ratios

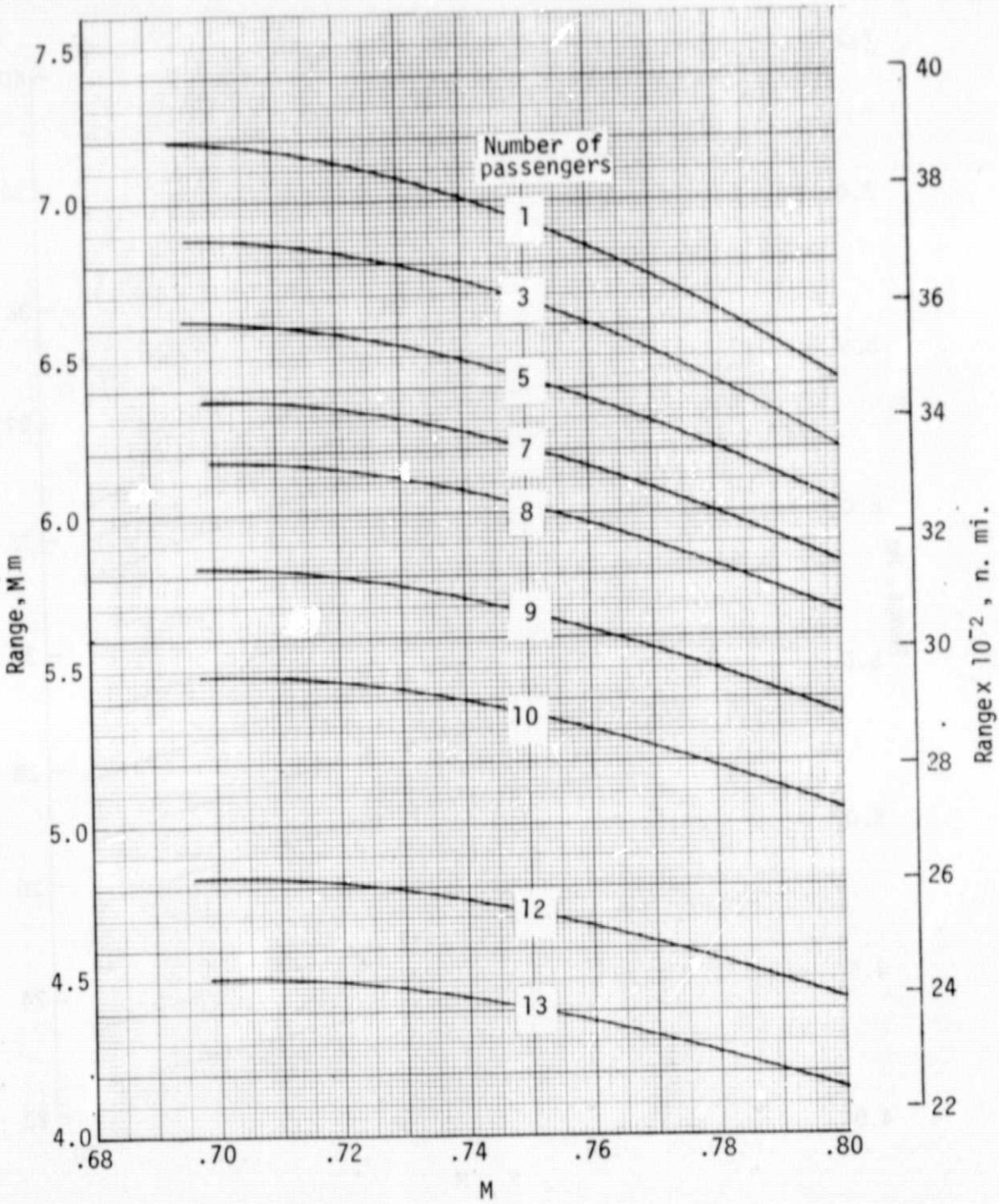


Figure 13. Range versus speed and no. of passengers for aircraft without LFC, with passenger accommodations adjusted for no. of pass. and fuel reserves for 45 min. additional flight time.

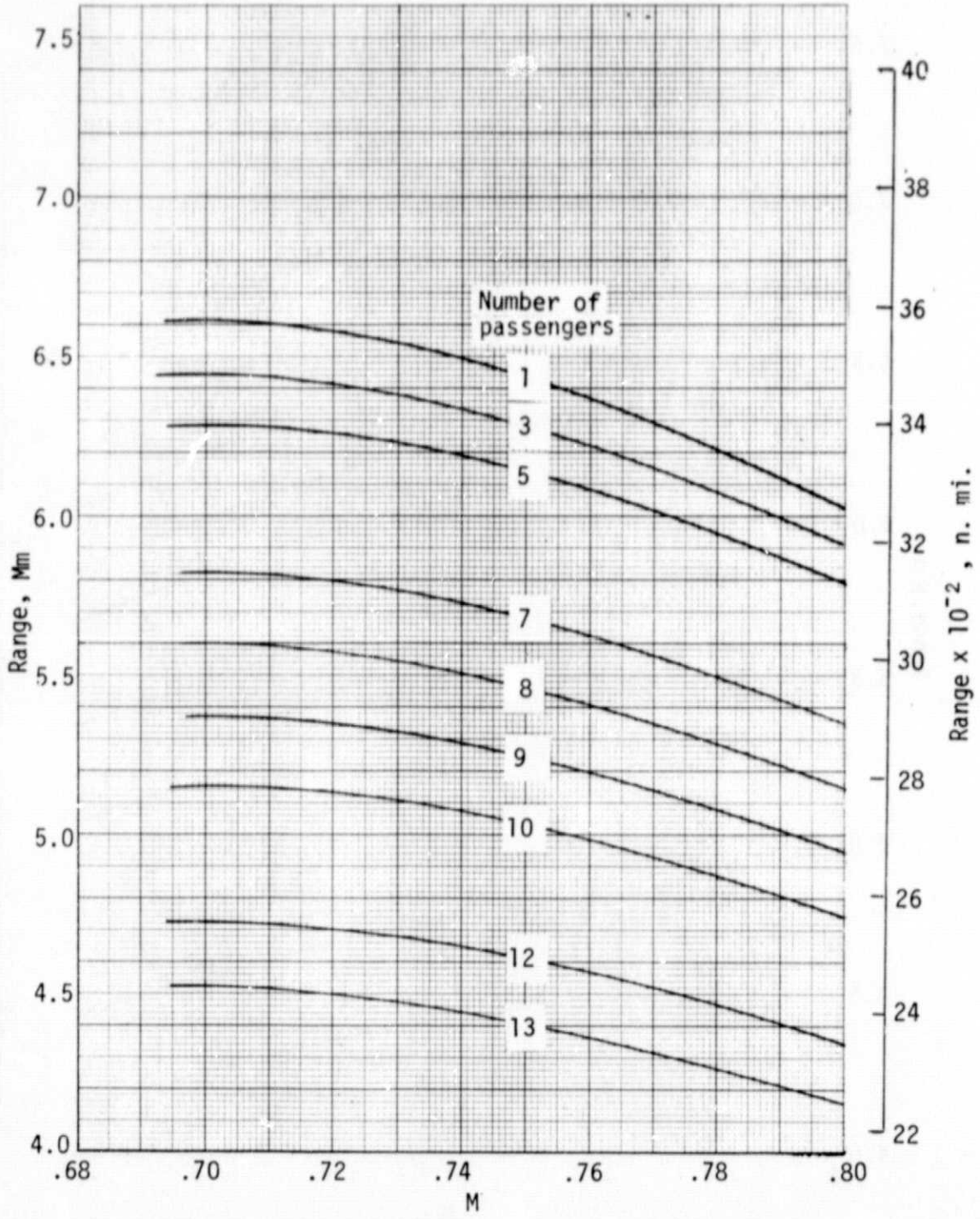


Figure 14. - Range versus speed and no. of passengers for aircraft without LFC, with passenger accommodations constant and equal that for 13 pass. and with fuel reserves for 45 min. additional flight time.

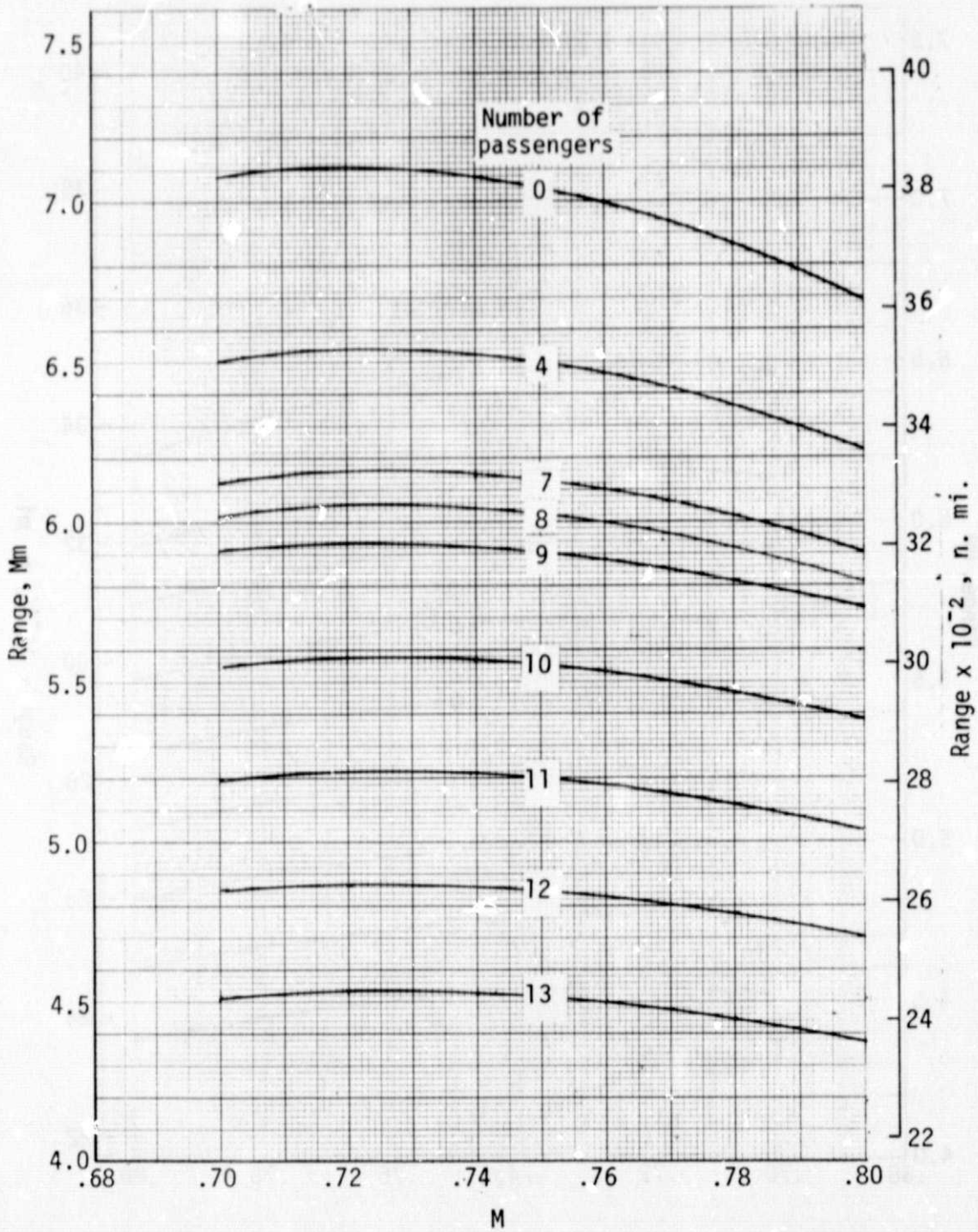


Figure 15. - Range versus speed and no. of passengers for aircraft with LFC, with passenger accommodations adjusted for no. of pass. and fuel reserves for 45 min. additional flight time.

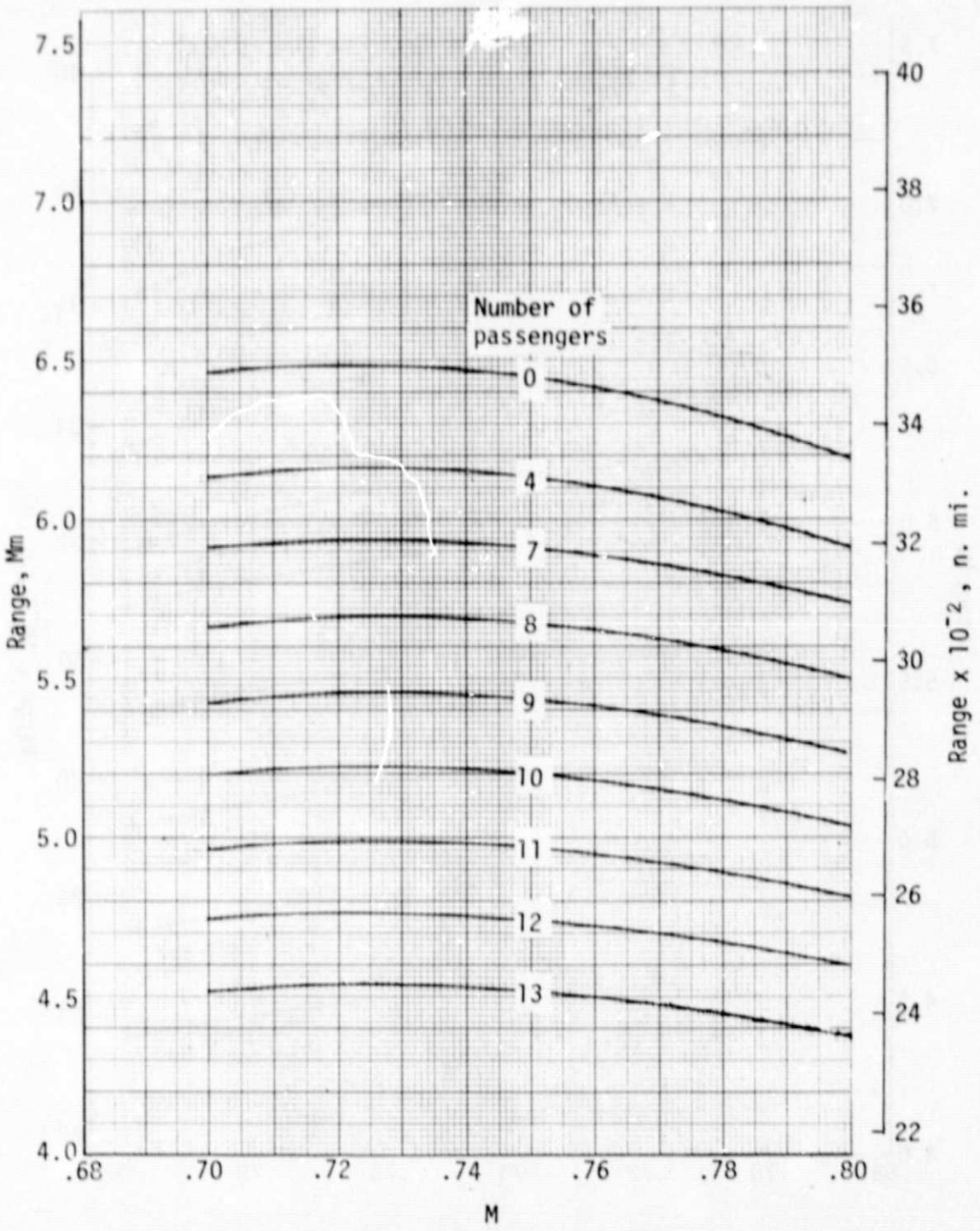


Figure 16. - Range versus speed and no. of passengers for aircraft with LFC, with passenger accommodations constant and equal that for 13 pass. and with fuel reserves for 45 min. additional flight time.

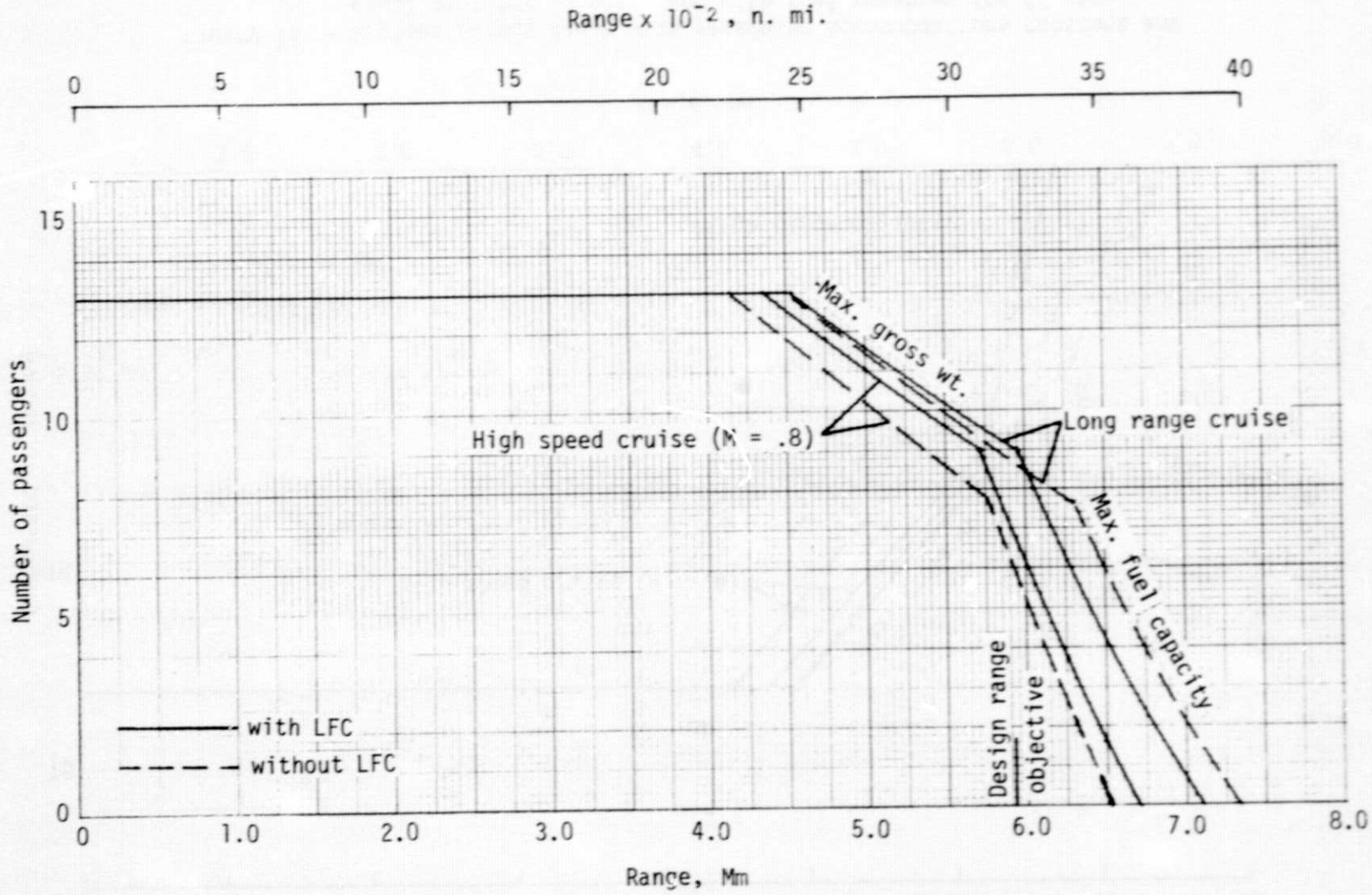


Figure 17. - Payload versus range with passenger accommodations adjusted for no. of passengers and fuel reserves for 45 min. additional flight time.

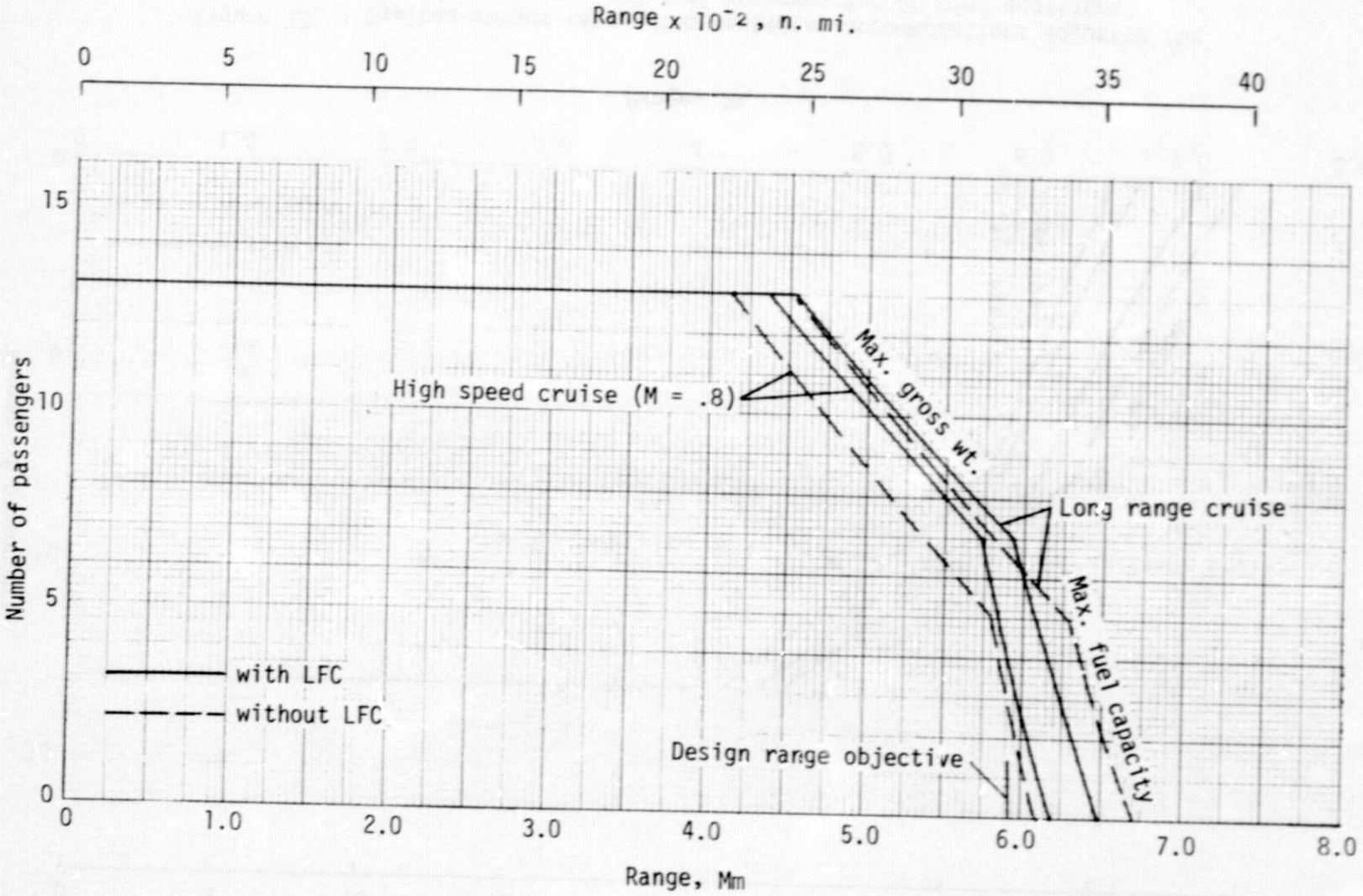


Figure 18. - Payload versus range with passenger accommodations constant and equal that for 13 pass. and with fuel reserves for 45 min. additional flight time.

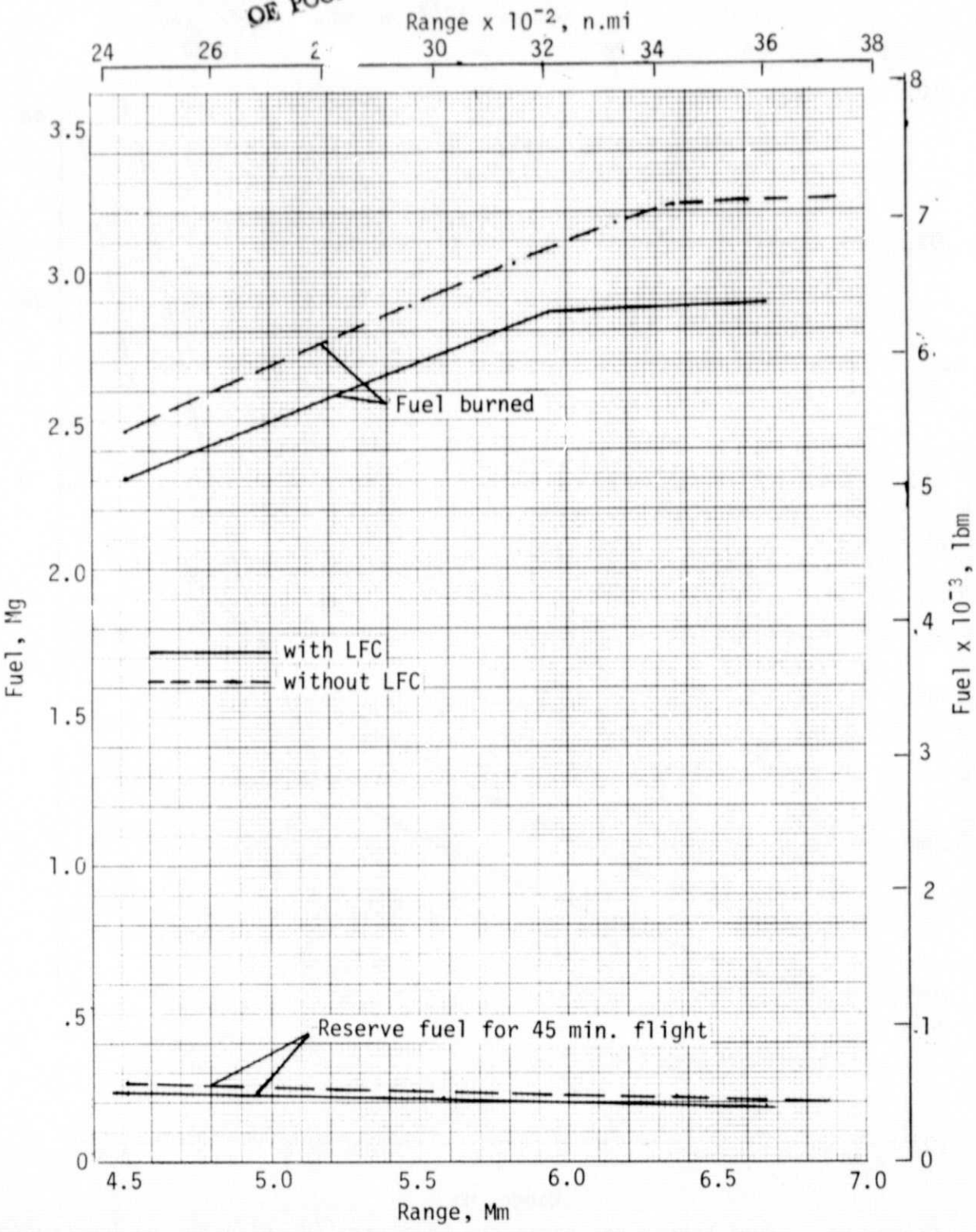


Figure 19. - Fuel burned and reserve fuel for long range cruise with passenger accommodations adjusted for no. of passengers.

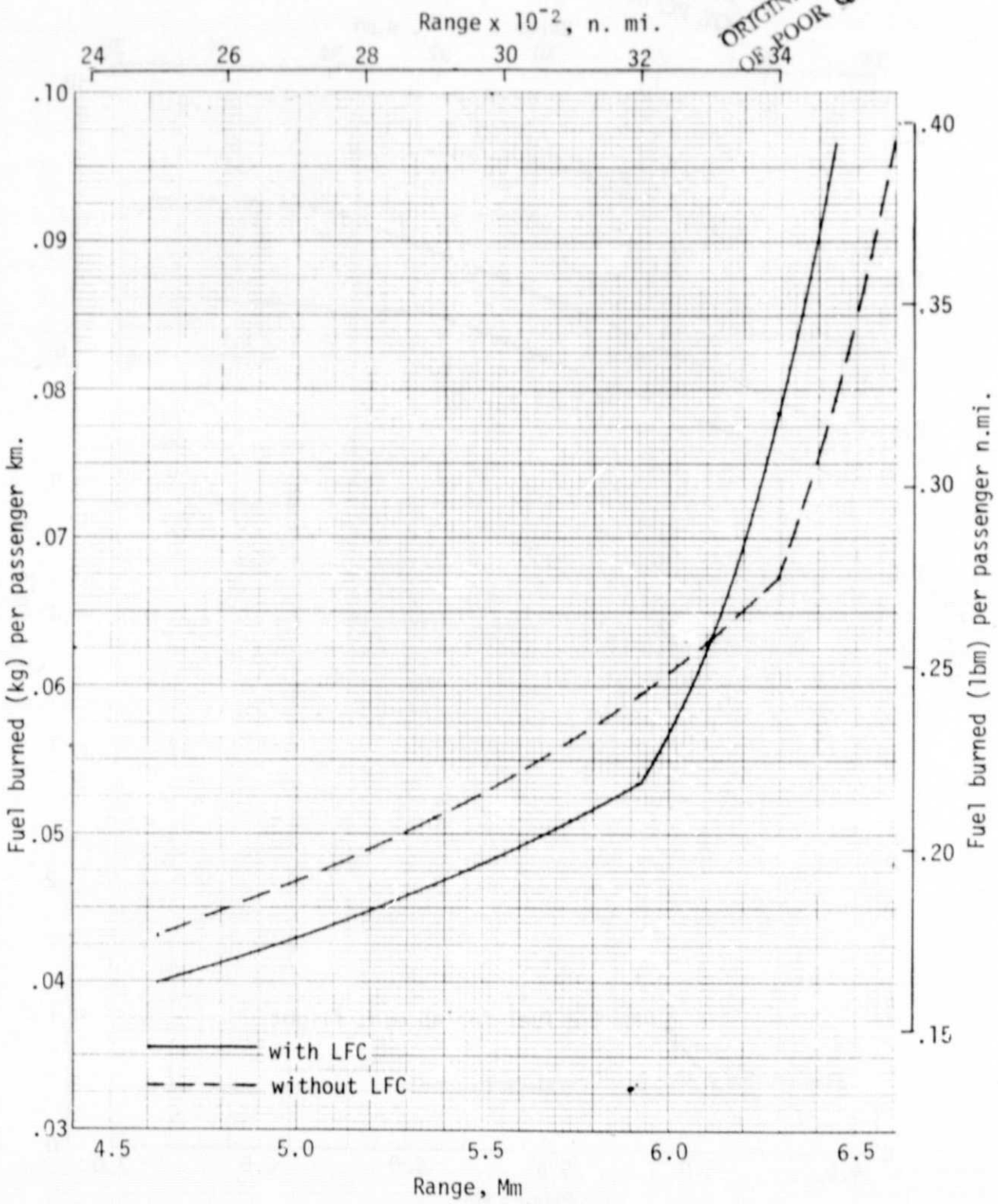


Figure 20. - Fuel burned per passenger kilometer (n. mi.) during long range cruise with passenger accommodations adjusted for no. of passengers.